Frontiers of Architectural Research 15 (2026) 705–728

Available online at www.sciencedirect.com

ScienceDirect

journal homepage: www.keaipublishing.com/foar

RESEARCH ARTICLE

Ranking and sorting the Pareto front in optimal shell structure design

Mohsen Vatandoost [a,c,*], Mahmood Golabchi [a], Ahmad Ekhlassi [b], Morteza Rahbar [b], Peter von Buelow [c]

[a] *Department of Architectural Technology, Faculty of Architecture, College of Fine Arts, University of Tehran, Tehran, Iran*
[b] *School of Architecture and Environmental Design, Iran University of Science and Technology, Tehran, Iran*
[c] *Taubman College of Architecture and Urban Planning, University of Michigan, Ann Arbor, MI, 48109, USA*

Received 5 March 2025; received in revised form 29 June 2025; accepted 18 July 2025

KEYWORDS
Multi-objective optimization (MOO);
Analytic hierarchy process (AHP);
Pareto front;
Decision-making;
Design space exploration;
Lightweight shell structures

Abstract The Pareto front is a collection of optimal solutions and trade-offs between objective functions without hierarchy. The challenge lies in selecting a single solution from this set for design development. This research utilizes a unique method that integrates multi-objective optimization (MOO) with the Analytic Hierarchy Process (AHP) method to score, rank, and sort the solutions of the Pareto front. First, a judgment matrix is created and evaluated based on the decision-maker's (DM) preferences over objective functions. Then, weight coefficients are derived from the judgment matrix to score and rank each solution in the Pareto front, allowing the sorting. The efficiency of this method was evaluated and discussed in two case studies of a complex, lightweight, continuous concrete shell structure, considering various design criteria that encompassed structural, acoustic, and energy performance. Additionally, the proposed method is compared with the weighted sum method. Combining MOO with the AHP enhances optimization and facilitates more effective interaction between the decision-maker and the optimal solution-finding process. This method enables a trade-off among criteria to solve a complex design problem. The DM's preferences guide the ranking process, and their active involvement ensures that the final solution aligns with the project's requirements and preferences.

* Corresponding author. Department of Architectural Technology, Faculty of Architecture, College of Fine Arts, University of Tehran, Tehran, Iran.
E-mail addresses: mohsen.vatandoost@ut.ac.ir, mohsenv@umich.edu (M. Vatandoost), golabchi@ut.ac.ir (M. Golabchi), ekhlassi@iust.ac.ir (A. Ekhlassi), rahbarm@iust.ac.ir (M. Rahbar), pvbuelow@umich.edu (P. von Buelow).
Peer review under the responsibility of Southeast University.

https://doi.org/10.1016/j.foar.2025.07.006

Nomenclature

Judgment matrix

n	number of rows in the judgment matrix
CI	coincidence indicator
CR	random consistency ratio
RI	average random consistency indicator
λ_{max}	The maximum value of the matrix eigenvalue
J	Judgment matrix
M_i	Multiplied elements in each row of the judgment matrix
w_i	weight coefficient
w_{i-norm}	Normalized weight coefficient

Optimization problem formulation

$\overrightarrow{X}$	Vector of variables
$\overrightarrow{f(\overrightarrow{X})}$	(Multi-objective) optimization function
$g_{j(\overrightarrow{X})}$	Unequal constraints
$h_{j(\overrightarrow{X})}$	Equal constraints
x_0, x_1, x_2	Control point on boundary curves
S_1, S_2, S_3	Defined control points on the shell surface
R_1 , R_2	The radius of the shell opening
t	Shell thickness
$f_{max-ranked}$	Maximum ranked solutions

1. Introduction

1.1. Problem statement

Navigating the complex field of multi-objective optimization can be challenging, yet it is essential for making informed and balanced decisions. Regarding multi-objective optimization for continuous lightweight concrete shell structures, the key question is how to choose a solution from the Pareto optimal set for design development. Utilizing multi-objective optimization provides a set of optimal solutions known as the Pareto front. These solutions are superior to others in the solution space but have yet to be ranked against each other (Crespino et al., 2024). For instance, refer to Fig. 1, which indicates the Pareto front provided by Pugnale et al. (2018) for the optimal shell design based on structural and acoustic performance. There are several candidate solutions (bold black dots) that can be selected as the final solution. Similarly, in research by Vatandoost et al. (2024b), as depicted in Fig. 2, the provided Pareto front for the optimal design of lightweight shell structures shows a tradeoff between weight, deflection, and strain energy. All of these solutions could be considered optimal designs. The question is how to select a solution from this set of optimal options for design development. This decision is primarily based on the architect's or decision maker's engineering judgment and experience. Some researchers have suggested utilizing the weighted sum method (Gunantara and Ai, 2018; Kumar et al., 2021; Lin et al., 2017), which merges the objective functions with a weight factor. This method is intended to simplify the optimization and transform the multi-objective optimization into a single-objective optimization. However, a single global solution is not guaranteed, and often current multi-objective algorithms cannot converge with a single global solution (Deb et al., 2016; Kim and de Weck, 2004).

Another method to address this problem is to allow the DM to interact with evolutionary algorithms (Ha and Carstensen, 2023; Li et al., 2023; Ponsi et al., 2021) and steer the exploration of the design space. Mueller et al. (2015) proposed a workflow that allows the DM to interact during the design process and optimization by determining the evolutionary parameters of mutation rate, generation size, and parent selection. In this method DM can consider both quantitative and qualitative goals. However, this method does not guarantee convergence to a global optimum. Additionally, a study by Xiao et al. (2023) introduces a phased synergistic method (PSM), which combines existing design tools and broadens their optimization scope through hierarchical iterations of design variables. While this method is useful for controlling the diversity of design solutions and steering the design toward the quantitative aspect, it cannot assist in picking (finding) a single final optimal solution in multi-objective optimization, mainly when numerous criteria are considered in the optimization.

Other methods include TOPSIS (Technique for Order of Preference by Similarity to Ideal Solution), which selects the solution closest to the ideal point and farthest from the non-ideal point (El-Bayeh et al., 2021; Kookalani et al., 2021; Yu et al., 2024). Moreover, LINMAP (Linear Programming for Multidimensional Analysis of Preferences) calculates the best trade-off solution by determining the normalized distance of each point on the Pareto front from an unobtainable ideal point. The solution with the minimal normalized distance is the best (Talaei and Sangin, 2024; Zihao et al., 2024). Prior methods in systematically selecting the most suitable solution from the Pareto front are summarized and compared in Table 1.

The Weighted Sum Method (WSM) simplifies optimization but struggles with weight determination and convergence. TOPSIS is efficient and straightforward but requires precise input and is sensitive to normalization. LINMAP offers flexibility without predefined weights but may face computational challenges as the number of objectives increases. The design space exploration method allows decision-makers to influence design parameters but does not guarantee a global optimum. The Phased Synergistic Method (PSM) enhances design diversity but fails to pinpoint a single optimal solution.

In addition, Machine learning models, such as Supervised learning, Unsupervised learning, and reinforcement learning (Ayman et al., 2024; Özerol and Arslan Selçuk, 2023; Thai, 2022), are among the methods used in predicting optimal solutions. ML models can predict the optimal solution very quickly; however, achieving accuracy is particularly challenging, as it is highly dependent on the dataset's input parameters and data. Having set up such a complex model requires obtaining reliable datasets, training the ML algorithm, verifying its accuracy, and tuning the algorithm, which is a rigorous task.

Since the machine learning models excessively rely on the input data (Datasets), in one hand, for most cases, such as the optimal design of lightweight shell structures, such datasets are not yet available, nor have not been provided and do not exist, or it is not available and accessible (Ali et al., 2024). On

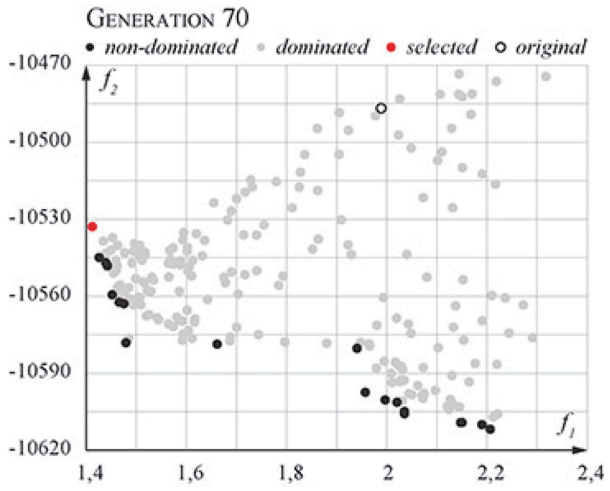

Fig. 1 The Pareto front of the optimal design of a shell, considering acoustic and structural objectives (black dots), adapted from Pugnale (2018).

the other hand, creating such a dataset for optimization is costly and time-consuming, and it may not be readily applicable to other research, remaining specific to that case. Moreover, training an ML model to predict the optimal design of lightweight shell structures when the datasets are limited is a highly challenging task, and achieving an accurate ML model is not easily attainable (Ayman et al., 2024; Özerol and Arslan Selçuk, 2023; Thai, 2022).

This research addresses the problem of ranking and sorting the Pareto front by a hybrid workflow that combines multi-objective optimization with the analytical hierarchy process (AHP). A systematic method is provided to allow the architect or decision-maker (DM) to collaborate more in the selection process. The architect will be able to sort the solutions in the Pareto front by shaping a judgment matrix created exclusively for each architectural design problem based on the DM preferences and project requirements (Podvezko, 2009), which will be utilized for ranking the solutions in the Pareto front.

1.2. Research objectives

The solutions on the Pareto front comprise a set of optimal solutions that are superior to others and not dominated by one another. To choose a single solution from this set for further design development, it is necessary to rank these solutions. Therefore, the objective of this research is to integrate multi-objective optimization (MOO) with the analytic hierarchy process (AHP) to rank and select an optimal solution from the Pareto front. The objectives and contributions of this research can be summarized as follows:

- Develop a unique method that integrates the analytic hierarchy process to score, rank, and sort solutions on the Pareto front.
- Improve optimization by systematically ranking solutions within the Pareto front.
- Demonstrate the method's efficiency through two case studies involving a complex, lightweight, continuous concrete shell structure, considering various design criteria, including structural, acoustic, and energy performance.
- Compare the results of the proposed method with those obtained using the weighted sum method in the same case study.
- Enable decision-makers to score, rank, and sort solutions based on their preferences, enhancing the decision-making process.
- Facilitate trade-offs among criteria to address complex design problems effectively.

2. Method

The workflow comprises three sequential phases: parametric modeling, optimization, and the implementation of a decision-making phase to determine the optimal design solutions (see Fig. 4).

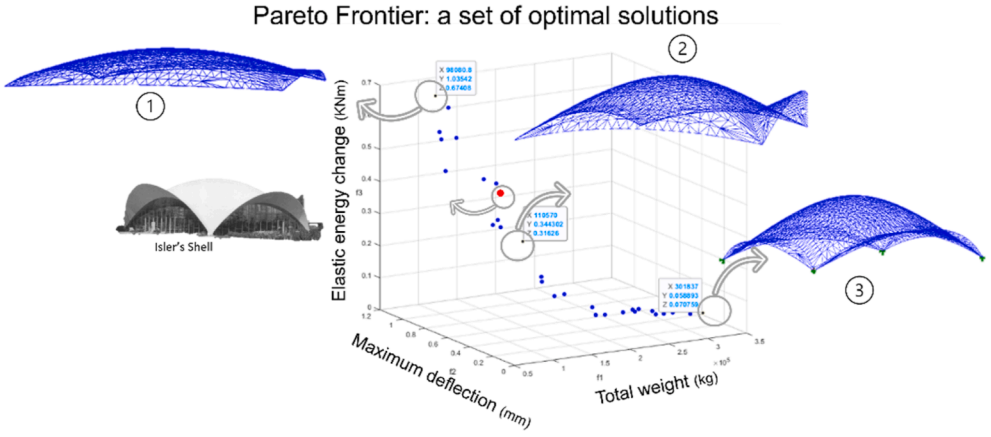

Fig. 2 The Pareto front for the optimal design of lightweight shell structures, highlighting the trade-off between weight, deflection, and strain energy, adapted from Vatandoost et al. (2024b).

Table 1 Overview of the methods for systematically selecting a solution from the Pareto front.

Method	Description	Advantages	Disadvantages/ limitations
Weighted sum method (WSM) (Gunantara and Ai, 2018; Kumar et al., 2021)	Merges the objective functions with a weight factor	Simplifying the optimization and transforming the multi-objective optimization into a single-objective optimization.	Determining the weight coefficients is challenging. This method will not always converge into a solution. Finding a global optimum is not guaranteed
TOPSIS (Technique for order of preference by similarity to ideal solution) (El-Bayeh et al., 2021; Lazar and Chithra, 2021; Yu et al., 2024)	Selecting the solution that is closest to the ideal point and farthest from the non-ideal point	Simplicity, computational efficiency, and the ability to handle multiple criteria	Requires precise numerical inputs and can be sensitive to the normalization process
LINMAP (Linear programming for multidimensional analysis of preferences) (Talaei and Sangin, 2024; Zihao et al., 2024)	Calculates the best trade-off solution by determining the normalized distance of each point on the pareto front from an unobtainable ideal point	Does not require predefined weights, allowing it to handle mixed information, including non-preference and preference information	As the number of objective functions increases, the linear program can grow significantly in size, potentially making computation infeasible due to memory or software limitations
Steer the exploration of the design space by DM (Ha and Carstensen, 2023; Li et al., 2023; Mueller and Ochsendorf, 2015)	DM will interact throughout the design process and optimization by determining the evolutionary parameters of mutation rate, generation size, and parent selection.	Control over the diversity of designs considered, the rate of convergence, and the multi-objective tradeoff between formulated quantitative goals. Can consider both quantitative and qualitative goals	The method does not guarantee convergence to a global optimum
Phased synergistic method (PSM) (Xiao et al., 2023)	Integrating existing design tools and expanding their optimization scope based on hierarchical iterations of design variables	This method is useful for controlling the diversity of design solutions and steering the design toward the quantitative aspect	It cannot assist in picking (finding) a single final optimal solution in multi-objective optimization
Machine learning based methods	ML models can "predict" the optimal solution quickly	ML models are speedy and do not rely on calculation but on previous data.	It relies vastly on datasets; such datasets are not available nor acceptable in all cases. Setting up a reliable ML model is a rigorous task. Achieving accuracy is challenging

Table 1 (*continued*)

Method	Description	Advantages	Disadvantages/ limitations
Integration of the AHP method (this manuscript)	MOO will determine the pareto front, and the solutions in the pareto front will be ranked and sorted by the AHP method and based on the DM's preferences.	Ranking the pareto front, which contains all the optimal (non-dominated) solutions. A ranking will be derived that reflects the decision-makers' priorities among the various objectives.	Has not yet been identified (see Section 4.8.)

2.1. Integrating multi-objective optimization with analytic hierarchy process

AHP is an established multi-criteria decision-making (MCDM) tool. It is a proven method that helps break down complex problems into smaller, more manageable parts by comparing and weighing the different criteria involved in a decision (Andreolli et al., 2022; Saaty, 1987). Using the AHP method, options and alternatives are prioritized based on objective criteria, resulting in more effective outcomes (Podvezko, 2009; Teknomo, 2006; Yu et al., 2018). Therefore, to enable architects or DM to interact with the process of choosing the fitness solutions, a novel method is proposed that links MOO with the AHP method. This process involves creating a judgment matrix, verifying its consistency, calculating weight coefficients, and ranking solutions based on the goal-level scores calculated for each solution (Fig. 5).

2.2. Judgment matrix

A judgment matrix, also known as a comparison matrix, is organized based on the relationships between various criteria or objectives. In this matrix, each column corresponds to an objective function, and the rows are arranged in the same order, see Eq. (1) (Banti and Krawczyk, 2024; Hou et al., 2023). For example, the element α_{12} located in row 1 and column 2 represents the relationship between objectives 1 and 2. Conversely, the element α_{21} in row 2 and column 1 indicates the relationship between objectives 2 and 1, which is equal to $1/\alpha_{12}$ as described in Eq. (2) (Sangiorgio et al., 2020).

$$\begin{array}{c} \\ \text{Objective}-1 \\ \cdots \\ \text{Objective}-n \end{array} \begin{array}{c} \begin{array}{ccc} \text{Objective}-1 & \cdots & \text{Objective}-n \end{array} \\ \begin{bmatrix} \alpha_{11} & \cdots & \alpha_{1n} \\ \vdots & \ddots & \vdots \\ \alpha_{n1} & \cdots & \alpha_{nn} \end{bmatrix} \end{array} \tag{1}$$

The relationship between elements of the matrix:

$$\alpha_{ij} = \frac{1}{\alpha_{ji}}. \tag{2}$$

The grading of the judgment matrix elements (objective functions) follows the guidelines provided in Table 2 (Mushtaha et al., 2020).

Additionally, Eq. (2) indicates that the elements within the judgment matrix are reciprocal. Determining the relationships between the objectives enables the construction of the entire matrix, as the elements are reciprocal (Guo et al., 2022; Xing et al., 2025). For example, if objective function 1 is considered of moderate importance compared to objective function 2, the value of α_{12} will be assigned 3 based on Table 2, Consequently, α_{12} would be 1/3. Furthermore, the diagonal elements of this matrix are always set to one, as they represent the relationship of an objective with itself.

When three objective functions are considered, the judgment matrix is represented as a three-by-three matrix (Eq. (3)). In this example, the user has determined that Objective 2 is "moderately important" compared to Objective 1, resulting in a matrix value of 3. Because the values in this matrix are reciprocal, the relationship between Objective 1 and Objective 2 is represented in row one and column two as one-third.

$$J = \begin{bmatrix} 1 & \frac{1}{3} & \frac{1}{9} \\ 3 & 1 & \frac{1}{7} \\ 9 & 7 & 1 \end{bmatrix}. \tag{3}$$

After creating the judgment matrix, its consistency ratio (*CR*) should be calculated based on Eq. (4) and verified (Saaty, 1987; Teknomo, 2006). The average random consistency indicator, RI, is provided in the literature based on the number of judgment matrix rows (*n*)

Table 2 Grading the elements of the judgment matrix according to their relationships.

Relation	Score
Equal important	1
Moderate important	3
Essential important	5
Very strong	7
Extreme	9

cited in Table 3. Therefore, the coincidence indicator (*CI*) and *CR* are calculated. The acceptable value for the consistency ratio is 1% or less. According to Teknomo (2006), the judgment matrix values must be updated if the consistency ratio exceeds 10% because it shows no consistency in the DM's preferences over objectives and the determined values.

$$\begin{cases} CI = \dfrac{\lambda_{max} - n}{n-1}, \\ CR = \dfrac{CI}{RI}. \end{cases} \tag{4}$$

n: number of rows in the judgment matrix ($n \times n$);
CI: Coincidence indicator (Calculate);
CR: Consistency ratio (Calculate);
RI: Average random consistency indicator (From Table 3);
λ_{max}: The maximum eigenvalue of the matrix (Calculate).

In the next step, weight coefficients (w_i) are calculated. The elements in each row of the judgment matrix are multiplied to obtain M_i, and then w_i is calculated using Eq. (5).

$$w_i = \sqrt[n]{M_i}. \tag{5}$$

i : the digit of each row;
n : number of rows in the judgment matrix;
M_i : Multiplied elements in row (i) of the matrix.

Then all the weight coefficients (w_i), should be normalized based on Eq. (6):

$$w_{i-\text{norm}} = \frac{w_i}{\sum_{i=0}^{n} w_i}. \tag{6}$$

w_i : the i^{th} weight coefficient.

Then, the values of the objective functions must be normalized. This normalization can be calculated similarly to Eq. (6) by dividing each objective function's value by the total sum of all values. Thus, by computing the scores of all the solutions in the Pareto front by employing weight coefficients, the solutions could be ranked and placed in order. Figure 5 summarizes the steps for creating the judgment matrix. Additionally, a Pseudocode is provided in Appendix for further clarification on the process and steps in the method. Moreover, a three-level hierarchical model (an AHP model) for the shell structure optimization is depicted in Fig. 3. Here, the first layer is the goal layer, which is finding the optimal design. The second layer is the criteria layer, which contains criteria (objective functions), and the third layer is alternatives (possible solutions).

Table 3 Average random consistency indicator values (*RI*) are based on the number of objective functions (n) (Teknomo, 2006).

n	1	2	3	4	5	6	7	8	9
RI	0.00	0.00	0.58	0.90	1.12	1.24	1.32	1.41	1.45

3. Application

Numerical examples are provided to demonstrate the effectiveness of the proposed method. In these two case studies, the aim is to optimize the topology and thickness of a lightweight shell structure.

3.1. Case study I: ISLER naturtheater, grötzingen, Germany, year: 1977

This open-air, thin concrete shell, designed and built by Isler based on experimental tests and hanging model

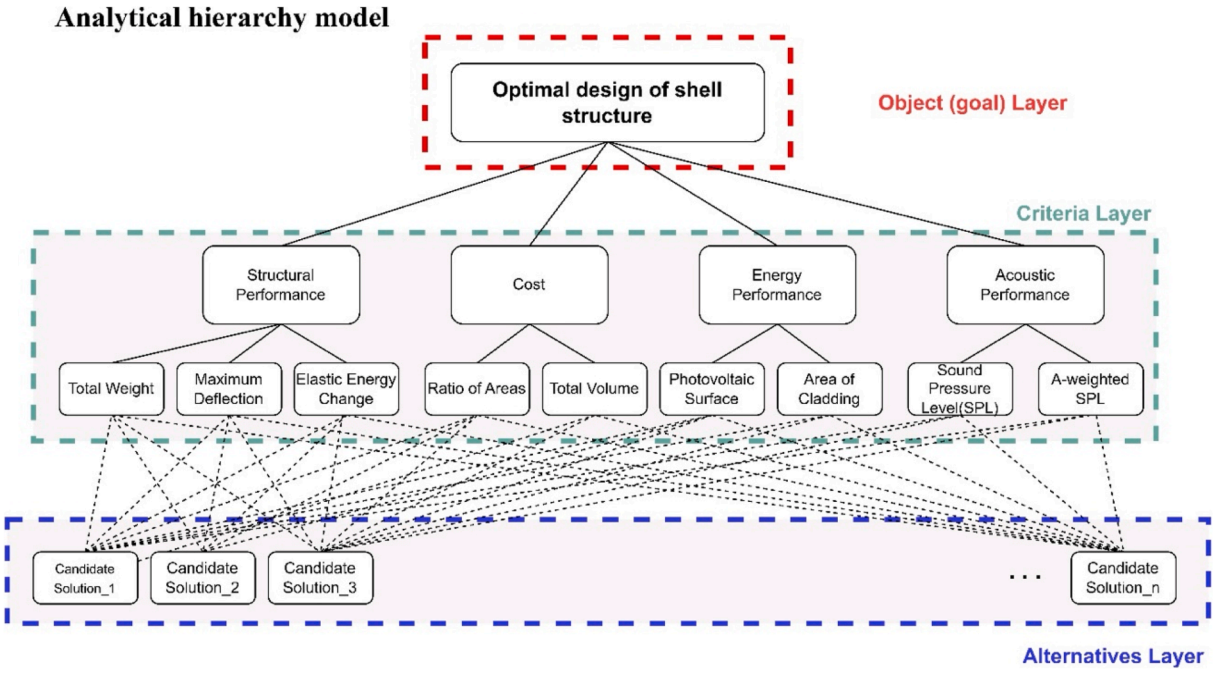

Fig. 3 A hierarchical model with three levels for optimizing the lightweight shell structure across multiple objectives.

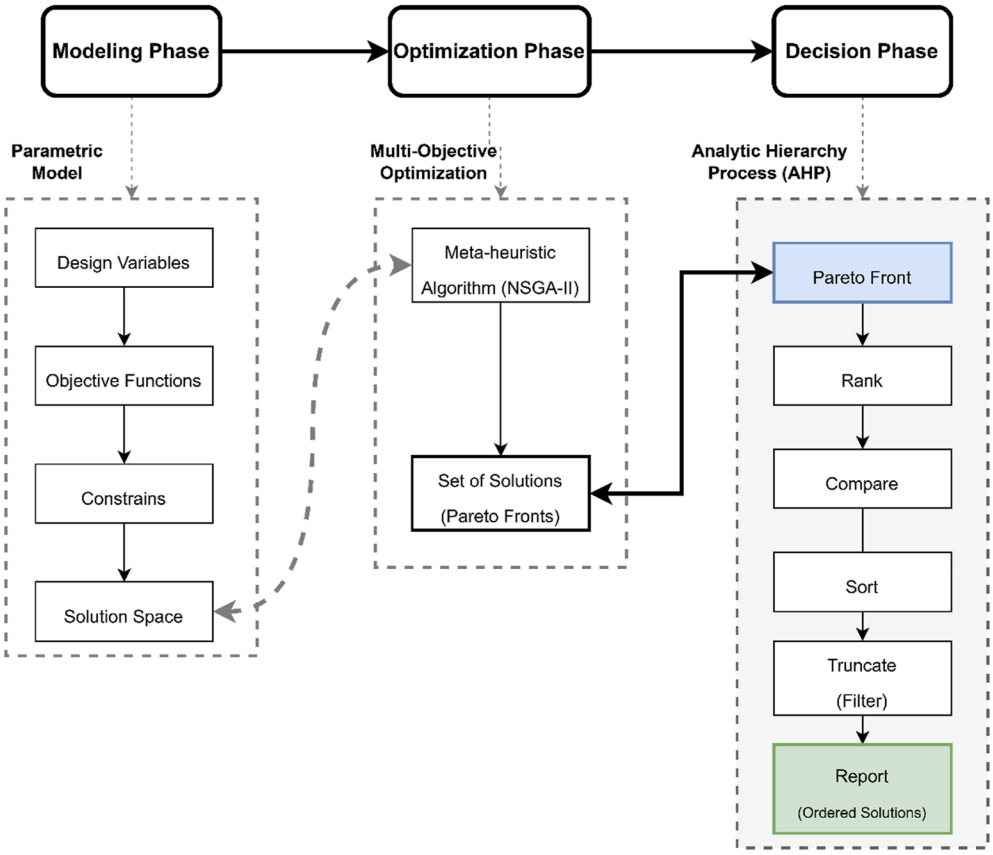

Fig. 4 The workflow for combining multi-objective optimization with AHP in the early stages of the design.

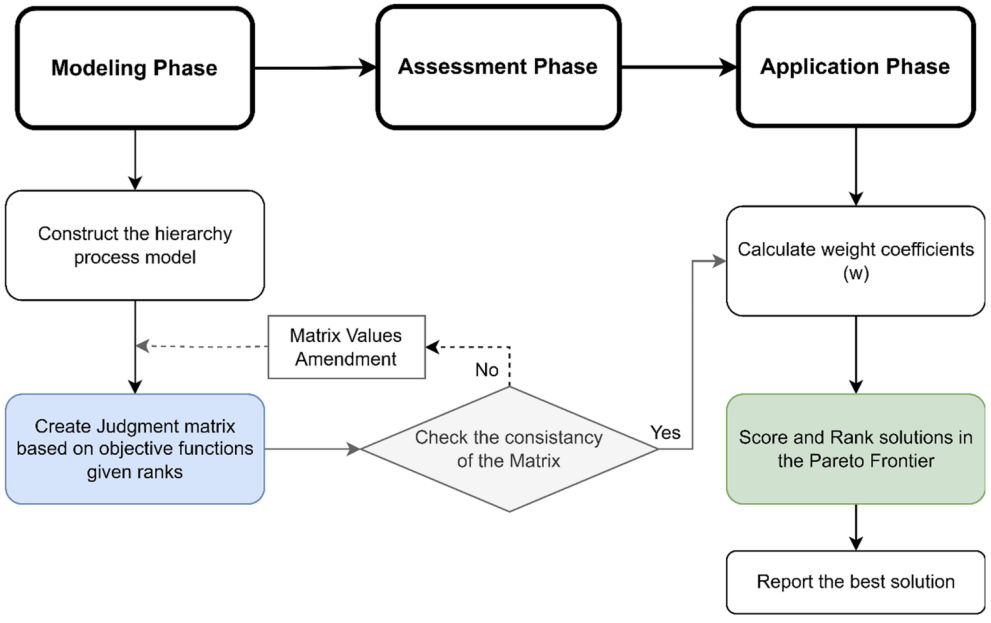

Fig. 5 Steps in Utilizing the AHP Method include constructing a judgment matrix, checking the consistency ratio, and determining the weight coefficients.

simulation (Baghdadi et al., 2020), was chosen as the base model. The resulting shell is a compression-only shell that is focused solely on structural performance (Goldbach and Lázaro, 2024; Mohsen Vatandoost et al., 2024). This pavilion, which is 28 m wide and 42 m long, has varying heights from 7.4 to a maximum of 10 m. The total area that is covered by the shell is 659 m^2. Additional design criteria were incorporated in this case study, including acoustic and energy performance. The results based on these criteria will be compared to the base model (the Isler shell). The details of this shell are depicted in Fig. 6.

3.1.1. Parametric model and variables

A network of boundary NURBS curves (Yan et al., 2022), Yu et al. (2022) represents the pavilion (Fig. 7). Each boundary NURBS curve is defined and controlled by a Bezier curve to provide a feasible topology for the shell. Ten points represent each boundary NURBS curve, but it is essential to indicate that to reduce the number of variables, for each curve, one control point is considered a variable, and the positions (z-direction) of the other points are mapped from the defined Bezier curvature (Vatandoost et al., 2024a). The x and y positions of the control points that create the shell are considered fixed. Therefore, nine independent variables are considered (Table 4).

3.1.2. Objective functions

Table 5 outlines the objective functions employed in the two case studies. In case study I, objective functions f_1 to f_3 were considered, while in case study II, functions f_1 to f_9 were utilized. For further clarification, additional details on how to measure each specific objective are provided in the appendix.

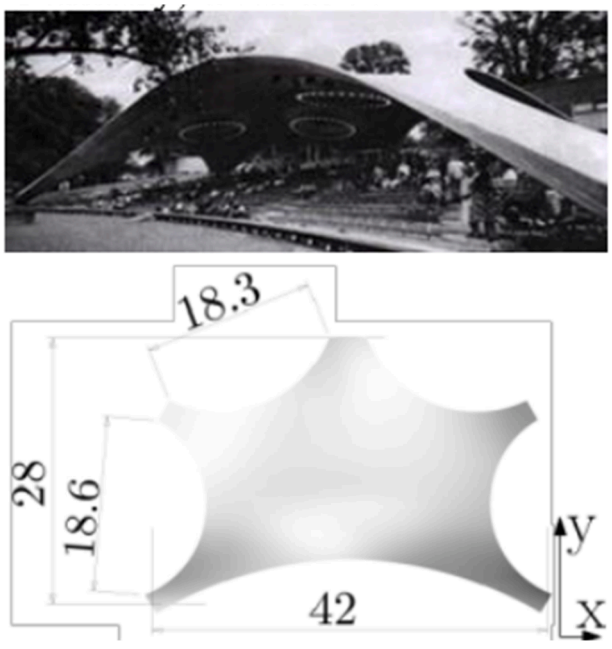

Fig. 6 Details of Isler's Naturtheater shell (base model) (Baghdadi et al., 2020).

3.1.3. Optimization formulation

In case study I, based on three considered criteria, f_1 to f_3, the optimization (Xu et al., 2024) could be formulated as Eq. (7):

$$\begin{aligned} &\text{Find} \quad \vec{X}, \text{which minimizes} \overrightarrow{f\left(\vec{X}\right)}, \\ &\vec{X} = [x_0, x_1, x_2, S_1, S_2, S_3, R_1, R_2, t], \\ &\overrightarrow{f\left(\vec{X}\right)} = \left[f_1\left(\vec{X}\right), f_2\left(\vec{X}\right), f_3\left(\vec{X}\right)\right]^T, \end{aligned} \tag{7}$$

$$\text{where} \quad f_1\left(\vec{X}\right) = v \cdot \gamma, \qquad f_2\left(\vec{X}\right) = \text{maximum deflection}, \qquad f_3\left(\vec{X}\right) = \frac{\sigma^2}{2E \times V}.$$

3.1.4. Integrating the analytical hierarchy process

For the case study I, the Pareto front by utilizing the NSGA-II method is represented in Fig. 8, where 50 solutions within the Pareto front are superior to all other candidate solutions. A judgment matrix is constructed which is a three-by-three matrix and is shown in Table 6. Additionally, this table highlights the relationships between the objectives in this case study. For instance, based on the constructed matrix, the Decision Maker (DM) considers the maximum deflection (f_2) to be 'extremely important' compared to the structure's total mass (f_1). This preference is reflected in row two and column 1 of the matrix, with a value of 9 assigned to this matrix element from Table 2.

Correspondingly, the entry in row one and column 2 should be set to one-ninth. Then, the consistency ratio (CR) of the matrix is checked based on Eq. (4), details are provided in Table 7. The consistency ratio is calculated as 9.52 ($CR = 9.52$) which is below 10% and acceptable.

In the next step, to calculate the weight coefficients (w_i), elements in each row of the judgment matrix should be multiplied to obtain M_i. Then w_i are calculated by Eq. (5). Finally, w_i are normalized based on Eq. (6) and reported below (Eq. (8)).

$$w_{i-\text{norm}} = [0.11398 \quad 0.81421 \quad 0.07180]^T. \tag{8}$$

It should be highlighted that the sum of the normalized weights ($w_{i-\text{norm}}$) must be one. Finally, each solution in the Pareto front will be scored using these weight coefficients. The values of objective functions must be normalized by dividing each value by the total sum of all objectives. For instance, one solution is brought out from the Pareto front, and the score is calculated (Table 8).

Consequently, by multiplying the normalized f and w matrixes, the score of each solution on the Pareto front will be computed. For instance, for the solution provided in Table 8, the score will be

$$f = [0.022805677 \quad 0.006778384 \quad 0.010842219];$$

$$w_{i-\text{norm}} = [0.11398 \quad 0.81421 \quad 0.07180]^T;$$

$$\text{Score} = f \cdot w_{i-\text{norm}} = 0.00889702.$$

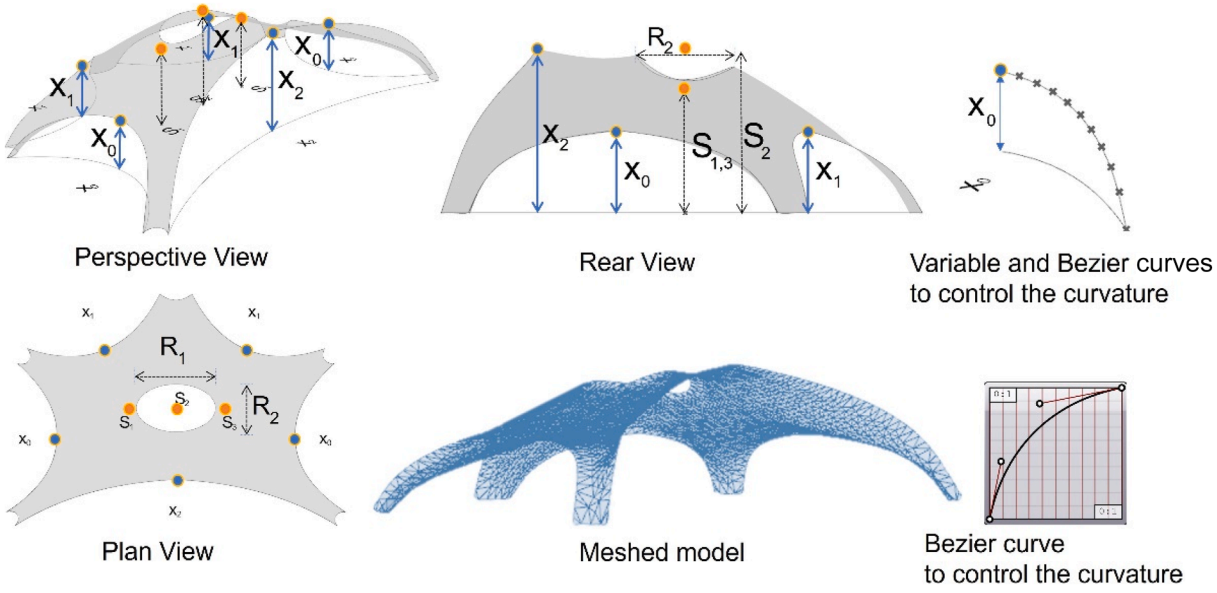

Fig. 7 The parametric model: a network of boundary NURBS curves representing the Pavilion, created based on Isler's Natur-theater shell.

Table 4 Variables in the parametric model.

Name	Description	Bound [Lb., Ub.]
x_0	z-coordinate of boundary NURBS curves (m)	[0.00, 10.00]
x_1		[0.00, 10.00]
x_2		[0.00, 10.00]
S_1	z-coordinate of the defined control point on the shell surface (m)	[5.00, 15.00]
S_2		[6.00, 15.00]
S_3		[5.00, 15.00]
R_1	Radius-1 of the opening (m)	[0.00, 5.00]
R_2	Radius-2 of the opening (m)	[0.00, 5.00]
t	Shell thickness (cm)	[6.00, 18.00]

x, S controling the shell topology in the z direction.
Ub: Upper bound, Lb: Lower bound.

Table 5 Objective functions utilized in the case studies.

Category	Objective function	Unit	Naming
Structure	Total mass	kg	f_1
	Maximum deflection	cm	f_2
	Elastic energy change	kN·m	f_3
Cost	The ratio of shell surface to the covering area	Unitless	f_4
	Total volume	m^3	f_6
Acoustic	Sound pressure level (SPL)	dB	f_7
	A-weighted SPL	dB	f_8
Energy	The surface area of the glazing	m^2	f_5
	Photovoltaic surface area (on the exterior surface)	m^2	f_9

Thus, by computing the scores of all the solutions in the Pareto front, the solutions could be ranked and placed in order. The best solution for this case study based on the constructed judgment matrix is depicted in Fig. 8. For the case study I, an additional judgment matrix is constructed, and the result is depicted in Fig. 8 for comparison.

3.2. Case study II: advanced application

To indicate the advantages of this method, in the following case, nine objective functions were considered simultaneously, making this a complex optimization problem. The optimization formulation for this case will be as Eq. (9).

$$\text{Find} \quad \vec{X}, \text{which minimizes} \overrightarrow{f\left(\vec{X}\right)};$$

$$\vec{X} = [x_0, x_1, x_2, S_1, S_2, S_3, R_1, R_2, t];$$

$$\overrightarrow{f\left(\vec{X}\right)} = \left[f_1\left(\vec{X}\right), f_2\left(\vec{X}\right), \ldots, f_9\left(\vec{X}\right)\right]^T.$$

Where

$$f_1\left(\vec{X}\right) = v \cdot \gamma;$$

$$f_2\left(\vec{X}\right) = \text{maximum deflection} \quad (\text{FEA Analysis});$$

$$f_3\left(\vec{X}\right) = \frac{\sigma^2}{2E \times V};$$

$$f_4\left(\vec{X}\right) = \frac{A_{\text{shell}}}{A_{\text{covering}}};$$

$$f_5\left(\vec{X}\right) = A_{\text{glazing}} = \sum_{i=1}^{n} A_i;$$

$$f_6\left(\vec{X}\right) = \text{Total volume} = A \cdot t;$$

$$f_7\left(\vec{X}\right) = -SPL_{\text{total}} = -\sum_{i=0}^{N} 10^{\frac{L_w - 20\ log_{10}(l_i) - 11}{10}};$$

$$f_8\left(\vec{X}\right) = -[A - \text{weighted sound pressure level}];$$

$$f_9\left(\vec{X}\right) = -0.4\, A_{\text{shell}}. \tag{9}$$

The $f_7(\vec{X})$, $f_8(\vec{X})$, and $f_9(\vec{X})$ are considered with a negative sign in the formula because it is intended to find the minimum of the whole $\overrightarrow{f(\vec{X})}$ while at the same time, the maximum amount for these three objective functions is desirable. The Pareto front, by employing the MOGA, NSGA-II, is provided in Fig. 10. Here are fifty solutions in the Pareto front. The first step in ranking and sorting the Pareto front by the AHP method is to construct a judgment matrix which is presented in Table 9.

In this judgment matrix, DM prefers a solution emphasizing the total weight (f_1), extremely *important* over the photovoltaic surface area (f_9) (row one, column 9 of the judgment Matrix-1).

Similarly, based on this matrix, DM's prefer deflection (f_2) as "extremely" important over the photovoltaic surface (f_9); refer to row two and column 9. Additionally, DM's preference for total weight (f_1) is "moderate" in importance over ratio (f_4), SPL (f_7), and A-weighted SPL (f_8), as reflected in this matrix. The judgment matrix's constancy ratio (*CR*) is calculated as 7.86, less than 10%, and hence is acceptable (Table 10). Then, the weight coefficients are calculated (Table 11). Then, all fifty solutions in the Pareto front based on these weight coefficients (Table 11) are scored. The best-ranked solution based on this judgment matrix is depicted in Fig. 10.

Another judgment matrix is constructed to compare the results (Table 12). In this matrix, DM's preference is toward a solution by putting "extreme" importance on the total volume (f_6) of the shell over acoustic performances (f_7, f_8) and photovoltaic surface (f_9). Please refer to rows six and columns 7, 8, and 9 of the judgment Matrix-2 in Table 12. Similarly, based on row six of this matrix, DM's preferred total volume (f_6) over total weight (f_1), deflection (f_2), and elastic energy change (f_3) are "extremely" important. In addition, DM prefers the total area of cladding (f_5) to be "moderately" important over f_1, f_2, and f_3. All other relations between objectives were determined to be of equal importance. The consistency ratio (*CR*) of this matrix is 8.85%, which is below 10% and is acceptable. The relevant weight coefficients are calculated and provided in Table 13.

4. Results and discussion

This study proposed a unique approach combining multi-objective optimization with the analytical hierarchy process to rank and sort the Pareto front. Two case studies were conducted to indicate the effectiveness of the

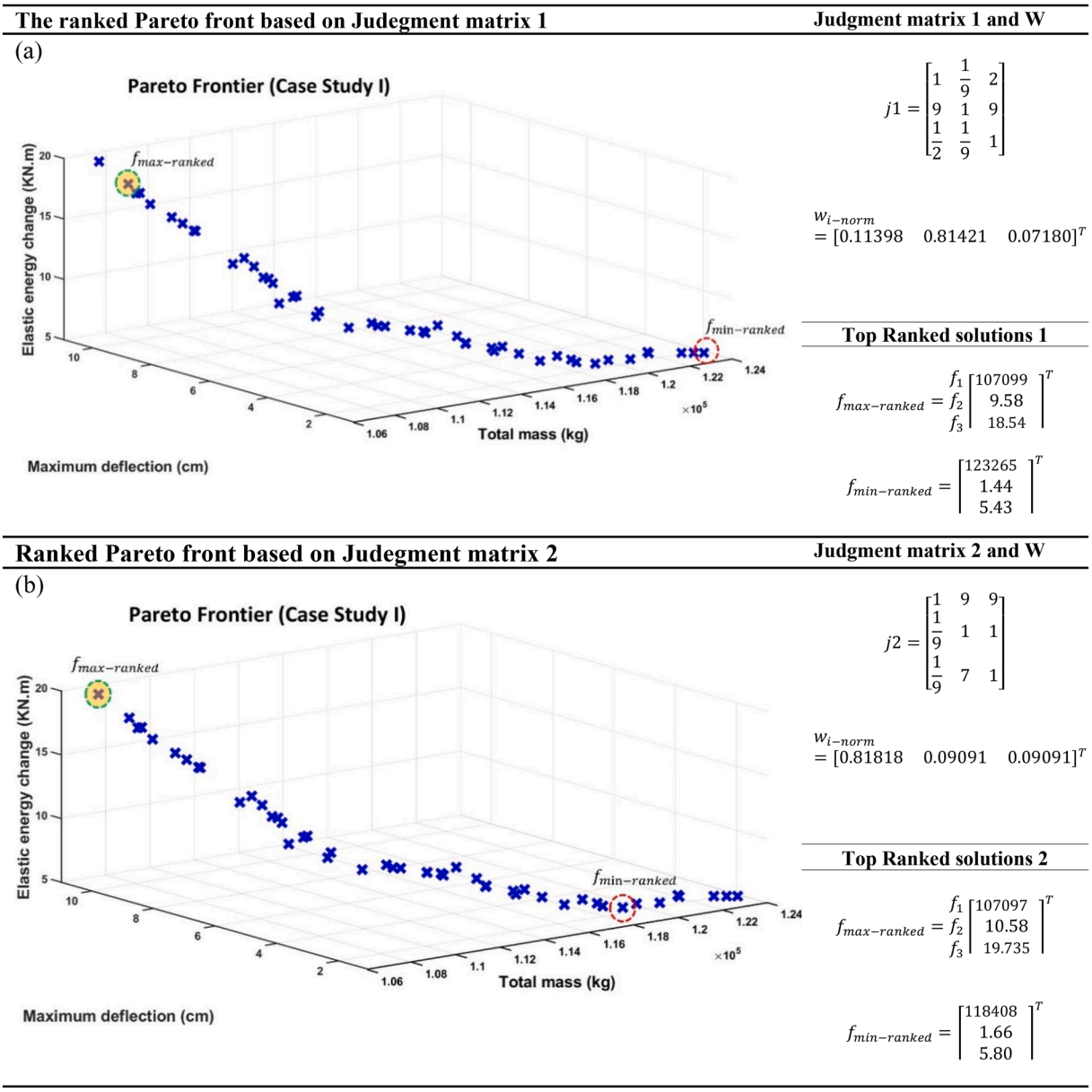

Fig. 8 Solutions of the Pareto front ranked by the AHP method: comparison of two different judgment matrices in Case study.

Table 6 Judgment matrix in case study I.

Objectives	Total mass	Maximum deflection	Elastic energy change
Total mass	**1**	$\frac{1}{9}$	2
Maximum deflection	9	**1**	9
Elastic energy change	$\frac{1}{2}$	$\frac{1}{9}$	**1**

proposed method in finding the optimal solution for continuous concrete shell structures by considering different criteria (objective functions) in the design.

4.1. Case study I

In the case study I, three objectives were considered: total mass, maximum deflection, and elastic energy change. The Pareto front is depicted in Fig. 8. There are solutions in this optimal set that represent different performances. For instance, the top-left solution in the Pareto front in this graph has the lowest total mass (f_1). In contrast, this solution has the highest elastic energy change (f_3), demonstrating its low stiffness compared to the solution in the bottom right of this graph, which contradicts the mentioned solution. This solution has the maximum total

Table 7 Assessment of the judgment matrix, case study I.

	Value	Reference
n	3	Number of rows
λ_{max}	3.11038961	Eq. (4)
CI	0.055194805	Eq. (4)
RI	0.58	Table 3
CR	0.095163457	Eq. (4)
Check if $CR < 10\%$.	9.52	Acceptable

Table 8 Actual and normalized values of the objective functions of an instance of the Pareto front.

	Actual measured value	Normalized calculated value
f_1	123264.81	0.022805677
f_2	1.44	0.006778384
f_3	5.43	0.010842219

Table 9 The judgment Matrix-1 in case study II.

	f_1	f_2	f_3	f_4	f_5	f_6	f_7	f_8	f_9
f_1	**1.00**	1.00	3.00	5.00	2.00	3.00	5.00	5.00	9.00
f_2	1.00	**1.00**	2.00	1.00	1.00	2.00	3.00	3.00	9.00
f_3	0.33	0.50	**1.00**	2.00	1.00	2.00	3.00	2.00	7.00
f_4	0.20	1.00	0.50	**1.00**	0.50	1.00	2.00	3.00	7.00
f_5	0.50	1.00	1.00	2.00	**1.00**	1.00	3.00	3.00	5.00
f_6	0.33	0.50	0.50	1.00	1.00	**1.00**	3.00	3.00	3.00
f_7	0.20	0.33	0.33	0.50	0.33	0.33	**1.00**	1.00	1.00
f_8	0.20	0.33	2.00	0.33	0.33	0.33	1.00	**1.00**	1.00
f_9	0.11	0.11	0.14	0.14	0.20	0.33	1.00	1.00	**1.00**

mass (f_1). The solutions in the Pareto front were normalized and then ranked based on the weight coefficients (Eq. (8)) extracted from judgment matrix. Figure 8 depicts the highest- and lowest-ranked solutions of the Pareto front. Therefore, the solutions in the Pareto front were sorted and ranked. For this case study, two distinct judgment matrices were considered for comparison (Figs. 8 and 9, Tables 14 and 15).

Table 10 Assessment of the judgment Matrix-1 in case study II.

	Value	Reference
n	9	Number of rows
λ_{max}	9.911796	Eq. (4)
CI	0.113975	Eq. (4)
RI	1.45	Table 2
CR	0.078603	Eq. 4
$CR < 10\%$?	7.860313	Check, acceptable if <10%

Table 11 Normalized weight coefficients in case study II by the judgment Matrix-1.

Name	Value
w_0	0.2642
w_1	0.1669
w_2	0.1271
w_3	0.0953
w_4	0.1340
w_5	0.0961
w_6	0.0417
w_7	0.0487
w_8	0.0259
Sum	**1.00**

4.2. Case study II

In case study II, nine objective functions were considered, which makes optimization a complex problem. The set of non-dominated solutions is presented in Fig. 10 as parallel plots. For case study II, the judgment Matrix-1 (Table 9) was constructed based on the DM's preferences over the objective functions and CR was calculated (Eq. (4), Table 10) as 7.8%, which is acceptable. Then, the weight coefficients were calculated and normalized; this is reflected in Table 11. Then, all fifty solutions in the Pareto front based on these weight coefficients were scored. The best-ranked solution based on this judgment matrix is depicted in Fig. 10, Table 16. To compare the maximum-ranked and minimum-ranked solutions based on the judgment Matrix-1, according to the graph provided in Fig. 10, the minimum-ranked solution was a solution that had better performance on f_1, f_2, f_3, f_4, f_5, and f_6 while having lower performance compared to the low-ranked solution on f_7, f_8, and f_9. Therefore, it can be concluded that if a solution with a minimum weight (f_1) is expected, one should pick the minimum ranked solution because when weight coefficients are determined in a way that the total weight of the structure is "extremely" important, therefore this judgment matrix will lead to a solution that has the almost highest weight from the Pareto front. Thus, in this case, the minimum-ranked solution should be considered, not the maximum-ranked solution. Additionally, an alternative judgment matrix (Table 12) was used to rank the solutions in case study II. The results based on this judgment matrices are depicted in Fig. 11. In addition, a detailed comparison of these two judgment matrices for picking the optimal solution is provided in Table 16.

4.3. Verifying the consistency of DM's selection (preferences)

The judgment matrix reflects the Decision Maker's (DM's) preferences over the objective functions. As mentioned earlier, to ensure that the elements of the matrix that show the relation between objective functions (based on Eq. (1),

Table 12 The judgment Matrix-2 in case study II.

	f_1	f_2	f_3	f_4	f_5	f_6	f_7	f_8	f_9
f_1	**1.00**	1.00	1.00	**0.33**	**0.33**	**0.11**	1.00	1.00	1.00
f_2	1.00	**1.00**	1.00	1.00	**0.33**	**0.11**	1.00	1.00	1.00
f_3	1.00	1.00	**1.00**	1.00	**0.33**	**0.11**	1.00	1.00	1.00
f_4	**3.00**	1.00	1.00	**1.00**	1.00	1.00	1.00	1.00	1.00
f_5	**3.00**	**3.00**	**3.00**	1.00	**1.00**	1.00	1.00	1.00	1.00
f_6	**9.00**	**9.00**	**9.00**	1.00	1.00	**1.00**	**9.00**	**9.00**	**9.00**
f_7	1.00	1.00	1.00	1.00	1.00	**0.11**	**1.00**	1.00	1.00
f_8	1.00	1.00	1.00	1.00	1.00	**0.11**	1.00	**1.00**	1.00
f_9	1.00	1.00	1.00	1.00	1.00	**0.11**	1.00	1.00	**1.00**

Table 13 Normalized weight coefficients in case study II for the judgment Matrix-2.

Name	Value
w_0	0.0545
w_1	0.0615
w_2	0.0614
w_3	0.1003
w_4	0.1282
w_5	0.3851
w_6	0.0696
w_7	0.0696
w_8	0.0696
Sum	**1.00**

Eq. (2) and Table 2) are determined in the same way, the consistency ratio (*CR*) of the judgment matrix needs to be checked. Based on the literature, *CR* should be less than 10% (Saaty, 1987; Teknomo, 2006). This means DM is consistent with his/her determination.

An example judgment matrix for case study I, where the user is inconsistent in their decision, is presented below:

$$J=\begin{bmatrix} 1 & \frac{1}{9} & 7 \\ 9 & 1 & 1 \\ \frac{1}{7} & 1 & 1 \end{bmatrix}, \quad CR=256\%, \text{not acceptable.}$$

Here, the *CR* is calculated as 256%, which is far greater than the acceptable 10%. Based on this matrix, first, the user determines the structure deflection to be "extremely important" over the total mass ($j_{21} = 9$) and indicates it is "Equal important" over the elastic energy change ($j_{23} = 1$) while determining the relation of the total mass "Very strong" to the elastic energy change ($j_{13} = 7$), which contradict with previous choice and highlights that DM is not consistent in his decision.

A quick fix is to alter $j_{12} = 9$, and as a result, $j_{21} = 1/9$. This will then have consistency with the choices, and the *CR* of the matrix is calculated as 1.2%. The modified matrix is provided below:

$$J=\begin{bmatrix} 1 & 9 & 7 \\ \frac{1}{9} & 1 & 1 \\ \frac{1}{7} & 1 & 1 \end{bmatrix}, \quad CR=1.2\%, \text{acceptable.}$$

4.4. The impact of DM's preferences on the final solution

Our observation and understanding of the proposed method suggest that potential biases may not arise if the decision-maker lacks sufficient experience, as the user's role in this proposed workflow is to determine preferences and hierarchize the criteria. Then, this workflow facilitates picking (selecting) an optimal solution from the Pareto front. There is no right or wrong solution; each solution on the Pareto front is superior to other potential solutions and is considered optimal. For instance, in the provided Pareto front in case study I, if the user's choices (judgment matrix) lead to selecting a different solution from the Pareto front (Fig. 8), all these solutions are still superior to other solutions and are considered optimal. The DM's preferences will only lead to (direct) the picking (selecting) one of these optimal solutions.

In other words, this proposed workflow facilitates selecting a solution based on preference and according to a scientific method; however, every solution on the Pareto front is still an optimized solution. What should be noted here is that if the users have the same preferences over the

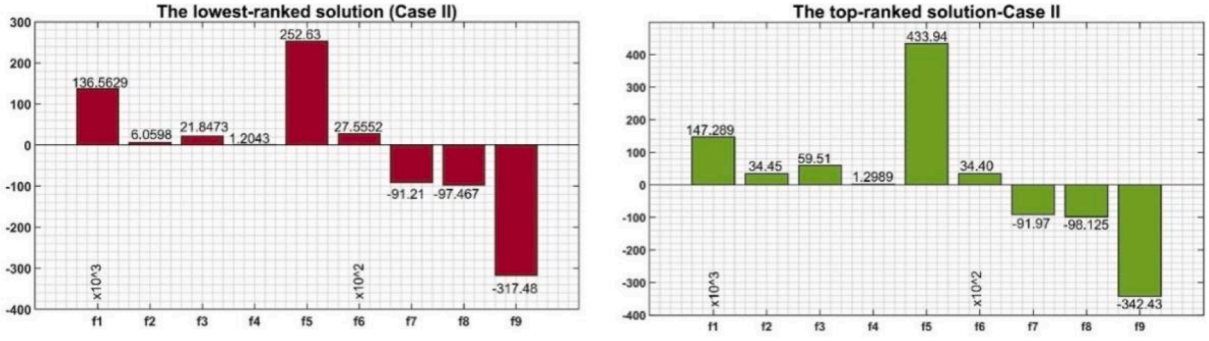

Fig. 9 The top-ranked and lowest-ranked solutions of the Pareto front are based on the chosen judgment matrix in case study II.

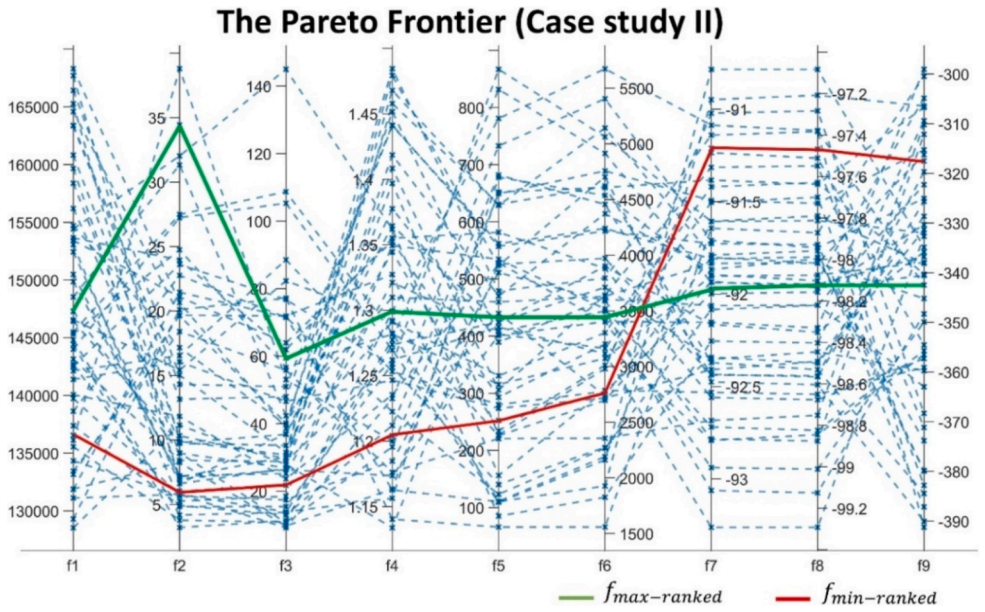

Fig. 10 The parallel plot of the Pareto front in case study II is based on judgment Matrix-1; The top-ranked and low-ranked solutions are highlighted.

Table 14 The final chosen solution from Pareto front in case study II based on two chosen judgment matrices.

Judgemnt matrix	$f_{min-ranked}$	$f_{max-ranked}$
Judgment Matrix-1 (refert to Table 9)	$f_{min-ranked} = [f_1\ 136562.9;\ f_2\ 6.0598;\ f_3\ 21.8473;\ f_4\ 1.2043;\ f_5\ 252.63;\ f_6\ 2755.52;\ f_7\ -91.21;\ f_8\ -97.467;\ f_9\ -317.48]^T$	$f_{max-ranked} = [f_1\ 147289.43;\ f_2\ 34.45;\ f_3\ 59.51;\ f_4\ 1.2989;\ f_5\ 433.94;\ f_6\ 3440.069;\ f_7\ -91.973119;\ f_8\ -98.1250;\ f_9\ -342.437]^T$

Table 15 The final chosen solution from Pareto front by constructing two different judgment matrices in case study I.

Category	Objective function		ISLER (base model)	Case study I: 3- Objective			
				Judgment matrix-1		Judgment matrix-2	
				$f_{min-ranked}$	$f_{max-ranked}$	$f_{min-ranked}$	$f_{max-ranked}$
Structure	Total Mass (kg)	f_1	130101.95	123265	107099	118408	107097
	Maximum deflection (mm)	f_2	6.160	1.44	9.58	1.66	10.58
	Elastic energy change (kN·m)	f_3	12.7722	5.43	18.54	5.80	19.73

criteria, they will end up picking the exact optimal solution from the Pareto front due to the same weights determined in the judgment matrix.

Moreover, as indicated in the method section, the consistency ratio (*CR*) should be kept below 10%, which is a very effective indicator for less experienced users because it makes them sure they are consistent with their preferences over the objective function, meaning the *CR* will be a high value if the user is not consistent within their preferences.

To study the effect of a DM's different choice (preference) over the relation of the objective functions and to examine this statement that different preferences might lead to different selecting, in case study I, we have randomly chosen 10 of the 125 possible judgment matrixes ($5^3 = 125$) and provided the weight coefficients based on the matrix, and

Table 16 The final chosen solution from Pareto front by constructing two different judgment matrices in case study II.

Category	Objective function		ISLER (base model)	Case study II: 9- Objective			
				Judgment Matrix-1		Judgment Matrix-2	
				$f_{\text{min ranked}}$	$f_{\text{max-ranked}}$	$f_{\text{min-ranked}}$	$f_{\text{max-ranked}}$
Structure	Total mass (kg)	f_1	130101.95	136562.9	147289.43	129266.47	149201.5
	Maximum deflection (mm)	f_2	6.160	6.059	34.45	20.08	9.50
	Elastic energy change (kN·m)	f_3	12.7722	21.85	59.51	77.06	19.74
Cost	The ratio of shell surface to covering the area (unitless)	f_4	1.1478	1.2043	1.2989	1.14	1.32
	Total volume (m^3)	f_5	4393.15	2755.52	3440.07	1554.557	5641.46
Acoustic	Sound pressure level (SPL) (dB)	f_6	−91.8592	−91.21	−91.9731	−91.6463	−92.0411
	A-weighted SPL (dB)	f_7	−98.08396	−97.467	−98.1250	−97.873	−98.2231
Energy	The surface area of the glazing (m^2)	f_8	704.6881	252.63	433.94	65.175	786.34
	Photovoltaic surface area (on the exterior surface) (m^2)	f_9	−302.600	−317.48	−342.437	−300.563	−347.023

finally, the solution that is picked from Pareto front is reported in Table 17 and Fig. 13. Our observations based on these results are summarized below.

The first observation, surprisingly, was that f_{max} was the same for all the judgment matrices. However, it might just be a coincidence and does not mean anything important, as further in this study, we have been able to obtain different f_{max} values based on different matrices and normalization methods (please see Table 18 and Fig. 14). At the same time, different f_{min} values were obtained using these various matrices in Table 17, which is sufficient to demonstrate that different preferences will result in different final selections.

Second, a glance at the calculated weight coefficient in Table 17 indicates that different matrices would result in

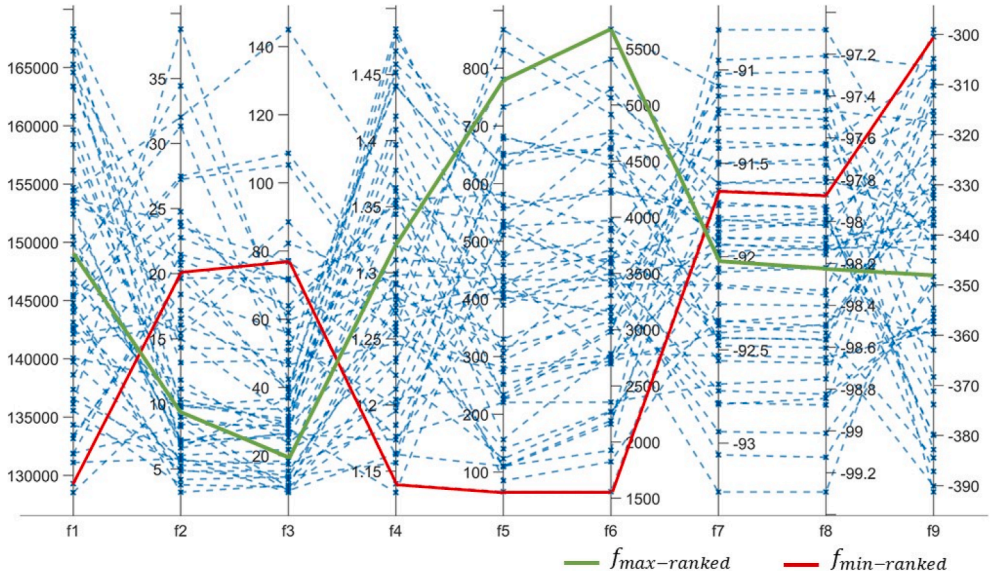

Fig. 11 The parallel plot of the Pareto front in case study II is based on **judgment Matrix-2**; The top-ranked and low-ranked solutions are highlighted.

Table 17 Different judgment matrixes for ranking the Pareto front in Case Study I to observe the impact of subjective preferences on the final solution (Also see Fig. 13).

Input			Result		
Judgment matrix	CR <10%	$w_{i-\text{norm}}$		$f_{\text{min-ranked}}$	$f_{\text{max-ranked}}$
$j1=\begin{bmatrix}1 & \frac{1}{9} & 2\\ 9 & 1 & 9\\ \frac{1}{2} & \frac{1}{9} & 1\end{bmatrix}$	9.52	$[0.11398 \quad 0.81421 \quad 0.07180]^T$	f_1 f_2 f_3	123265 1.44 5.43	107097 10.58 19.735
$j2=\begin{bmatrix}1 & 9 & 9\\ \frac{1}{9} & 1 & 1\\ \frac{1}{9} & 1 & 1\end{bmatrix}$	0	$[0.81818 \quad 0.09091 \quad 0.09091]^T$	f_1 f_2 f_3	118408 1.66 5.80	107097 10.58 19.735
$j3=\begin{bmatrix}1 & 9 & 3\\ \frac{1}{9} & 1 & \frac{1}{7}\\ \frac{1}{3} & 7 & 1\end{bmatrix}$	10.53 >10%	$[0.65535 \quad 0.05490 \quad 0.28974]^T$	f_1 f_2 f_3	118408 1.66 5.80	107097 10.58 19.735
$j4=\begin{bmatrix}1 & \frac{1}{2} & \frac{1}{2}\\ 2 & 1 & \frac{1}{2}\\ 2 & 2 & 1\end{bmatrix}$	5.23	$[0.19580 \quad 0.31081 \quad 0.49338]^T$	f_1 f_2 f_3	123264 1.66 5.43	107097 10.58 19.735
$j5=\begin{bmatrix}1 & 1 & 1\\ 1 & 1 & 1\\ 1 & 1 & 1\end{bmatrix}$	0	$[0.33333 \quad 0.33333 \quad 0.33333]^T$	f_1 f_2 f_3	122870 1.51 5.475	107097 10.58 19.735
$j6=\begin{bmatrix}1 & \frac{1}{2} & \frac{1}{7}\\ 2 & 1 & \frac{1}{5}\\ 7 & 5 & 1\end{bmatrix}$	2.12	$[0.09381 \quad 0.16659 \quad 0.73959]^T$	f_1 f_2 f_3	122870 1.51 5.475	107097 10.58 19.735
$j7=\begin{bmatrix}1 & 1 & 7\\ 1 & 1 & 7\\ \frac{1}{7} & \frac{1}{7} & 1\end{bmatrix}$	0	$[0.46667 \quad 0.46667 \quad 0.06667]^T$	f_1 f_2 f_3	118408 1.66 5.8	107097 10.58 19.735
$j8=\begin{bmatrix}1 & \frac{1}{5} & \frac{1}{3}\\ 5 & 1 & 3\\ 3 & \frac{1}{3} & 1\end{bmatrix}$	4.77	$[0.10473 \quad 0.63698 \quad 0.25828]^T$	f_1 f_2 f_3	122870 1.51 5.475	107097 10.58 19.735
$j9=\begin{bmatrix}1 & \frac{1}{9} & 7\\ 9 & 1 & 1\\ \frac{1}{7} & 1 & 1\end{bmatrix}$	256%, not acceptable	$[0.26107 \quad 0.59051 \quad 0.14841]^T$	f_1 f_2 f_3	122870 1.51 5.475	107097 10.58 19.735
$j10=\begin{bmatrix}1 & 9 & 7\\ \frac{1}{9} & 1 & 1\\ \frac{1}{7} & 1 & 1\end{bmatrix}$	1.2	$[0.79859 \quad 0.09648 \quad 0.10492]^T$	f_1 f_2 f_3	118408 1.66 5.8	107097 10.58 19.735

quite different weight coefficients. However, this did not lead to a significantly different final solution due to the established relationship between the objective functions related to this specific case. In other words, the values of the objective function are such that even different weight coefficients will not result in a hugely different and varied solution. This might be specific to this experience and not applicable to other cases, but it is something worth noting.

Third, among the judgment matrixes was an extreme case, *j*5, in which user preferences over all the objective functions were the same (equal important = 1). Of course, the *CR* was zero, in case the DM is very solid in his/her choice. The weight coefficients were the same, and the result was more toward the solution with the maximum mass (the objective function1, f_1).

Fourth, *j*9 was a judgment matrix in which the DM's choices were highly inconsistent, leading to a *CR* of 2%, which is far greater than the 10% acceptance limit. Nevertheless, this judgment matrix can pick a solution from the Pareto front, but it is probably just a random choice with no meaning, and it is not useful.

Fifth, another observation was that within *j*5 and *j*6, while different matrices were constructed, the same solution was selected by the method. This will likely happen many times when using this method, where the preferences are slightly different, and the composition of values (objective function) dominates the results.

Lastly, this requires further study to determine what effect choosing a different normalization method, for example, Min-Max Normalization instead of "Divide by Column Average Normalization," would have on the final choice. Currently, in this case, the f_1 has the most significant value, and it appears that the different weight objectives are unable to shift the combination of the objective functions to a different f_{max}. This will help determine whether this is the cause in this particular case; this is assessed in the following section (see Section 4.5).

4.5. The impact of the normalization method

To determine how the method of normalizing the objective functions in the Pareto front affects the final selected solution, three different strategies were implemented (N_1 to N_3; Eq. (6), Eq. (10), Eq. (11)). The results of implementing the two judgment matrices in Case Study I are compared in Table 18 and Fig. 14. The three normalization methods include:

N_1: (Divide by Column Average Normalization)

$$f_{i-\text{norm}} = \frac{f_i}{\sum_{i=0}^{n} f_i}. \quad \text{Repeated (page 5)}$$

N_2: (Min-Max Normalization)

$$f_{i-\text{norm}} = \frac{f_i - f_{\min}}{f_{\max} - f_{\min}}. \tag{10}$$

N_3: (Z-Score Normalization)

$$f_{i-\text{norm}} = \frac{f_i - \mu}{\sigma}. \tag{11}$$

f_i is the i^{th} objective function;

n is the total number of values of a single objective function;
μ is the mean of the feature (objective function);
σ is the standard deviation of the feature.

The normalization based on Eq. (6) (N_1) divides each value of the column bNy the total average of the column to normalize it, while normalization based on Eq. (10) (N_2) parametrizes the values between 0 and 1. The Z-Score normalization (N_3, Eq. (11)) Scales the values so that they have a mean of 0 and a standard deviation of 1 (Henderi et al., 2021).

Based on Table 18 and Fig. 14, our observation indicates that implementing j1 resulted in the same f_{max} across the three normalizing methods. In contrast, the f_{min} differed when utilizing N_2 and N_3 compared to N_1. However, both N_2 and N_3 found the same f_{min}. Additionally, by implementing *j*2, a completely different maximum solution, f_{max}, was obtained based on N_2 and N_3 in comparison to N_1, and again, it was similar in N_2 and N_3, showing a stronger bond between these two normalization methods. However, the minimum picked solution, f_{min}, was utterly different from each other by implementing N_1, N_2, and N_3.

This experience was conducted to show that the final picking solution is sensitive to the normalization method. It can be stated that without standardization, the model might prioritize an objective function because the values are significantly larger (in this case, the total mass compared to deflection and

Table 18 Study the final selected result while three different strategies for normalization of the values of the objective function in the Pareto front were implemented (N_1 to N_3).

Input					Result						
					N_1		N_2		N_3		
Judgment matrix	*CR* <10%	$w_{i-\text{norm}}$			$f_{\min-\text{ranked}}$	$f_{\max-\text{ranked}}$	$f_{\min-\text{ranked}}$	$f_{\max-\text{ranked}}$	$f_{\min-\text{ranked}}$	$f_{\max-\text{ranked}}$
$j1 = \begin{bmatrix} 1 & \frac{1}{9} & 2 \\ 9 & 1 & 9 \\ \frac{1}{2} & \frac{1}{9} & 1 \end{bmatrix}$	9.52	[0.11398	0.81421	0.07180]^T	f_1 122870 f_2 1.51 f_3 5.475	107097 10.58 19.735	118408 1.66 5.8	107097 10.58 19.735	118408 1.66 5.8	107097 10.58 19.735
$j2 = \begin{bmatrix} 1 & 9 & 9 \\ \frac{1}{9} & 1 & 1 \\ \frac{1}{9} & 1 & 1 \end{bmatrix}$	0	[0.81818	0.09091	0.09091]^T	f_1 118408 f_2 1.66 f_3 5.80	107097 10.58 19.735	107397 5.79 14.93	123265 1.66 5.43	108017 4.43 12.54	123265 1.66 5.43

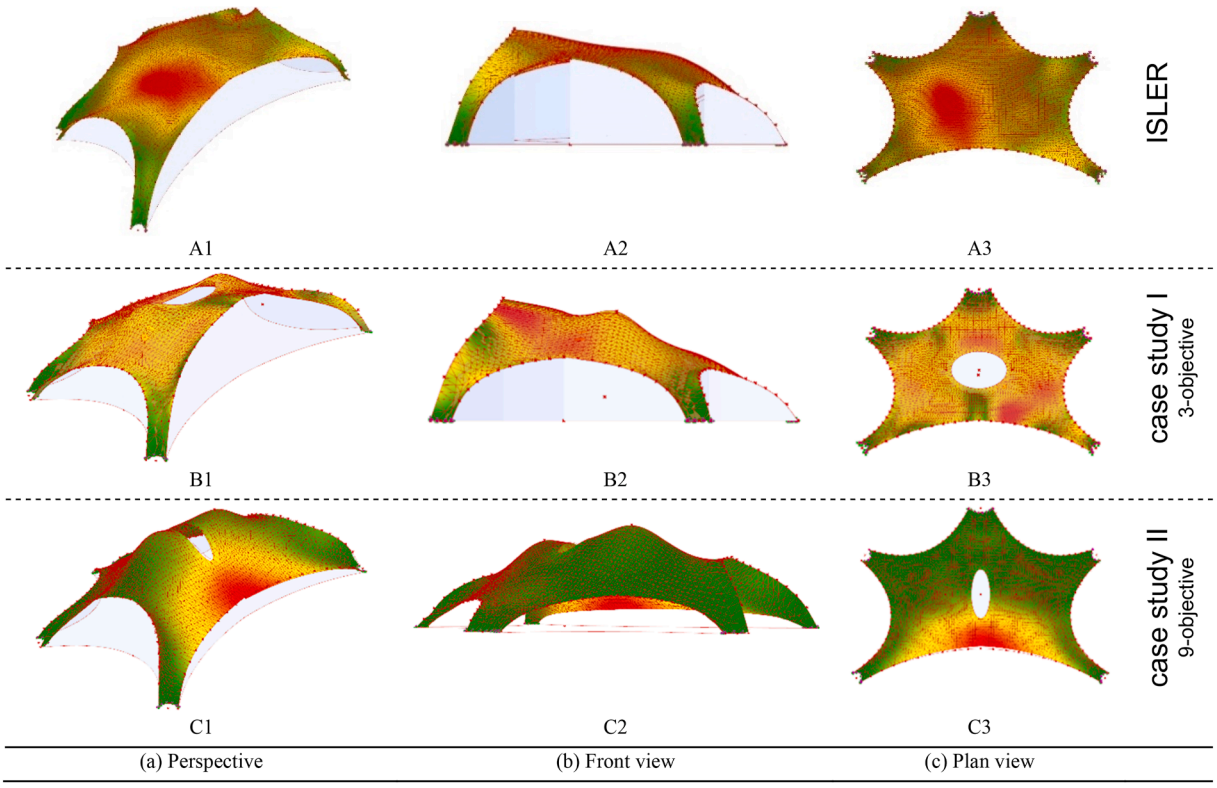

Fig. 12 The final best-chosen solution in case studies I and II, determined after scoring and ranking using the AHP method.

elastic energy change) than the other values (objective functions). By standardizing, the two features are brought to the same scale, allowing for a more balanced analysis.

Overall, we will not be able to settle a meaningful or solid conclusion based on this limited data and experience. More rigorous investigations are required to reveal the

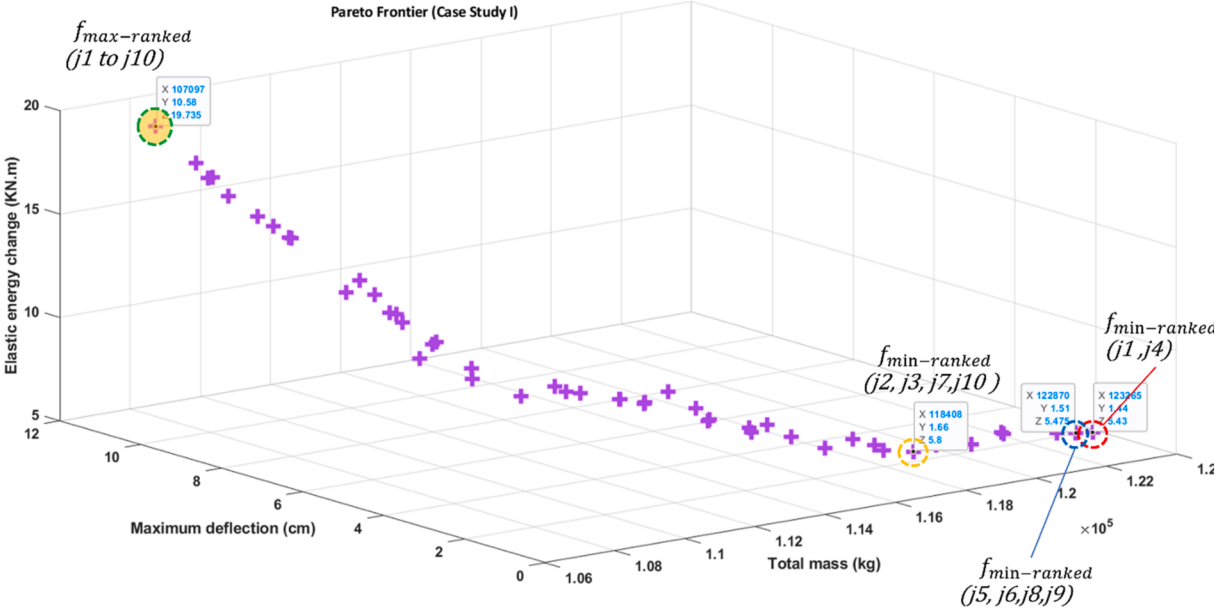

Fig. 13 The final best-chosen solution in case study I to study the impact of subjective preferences on the final solution (see also Table 17).

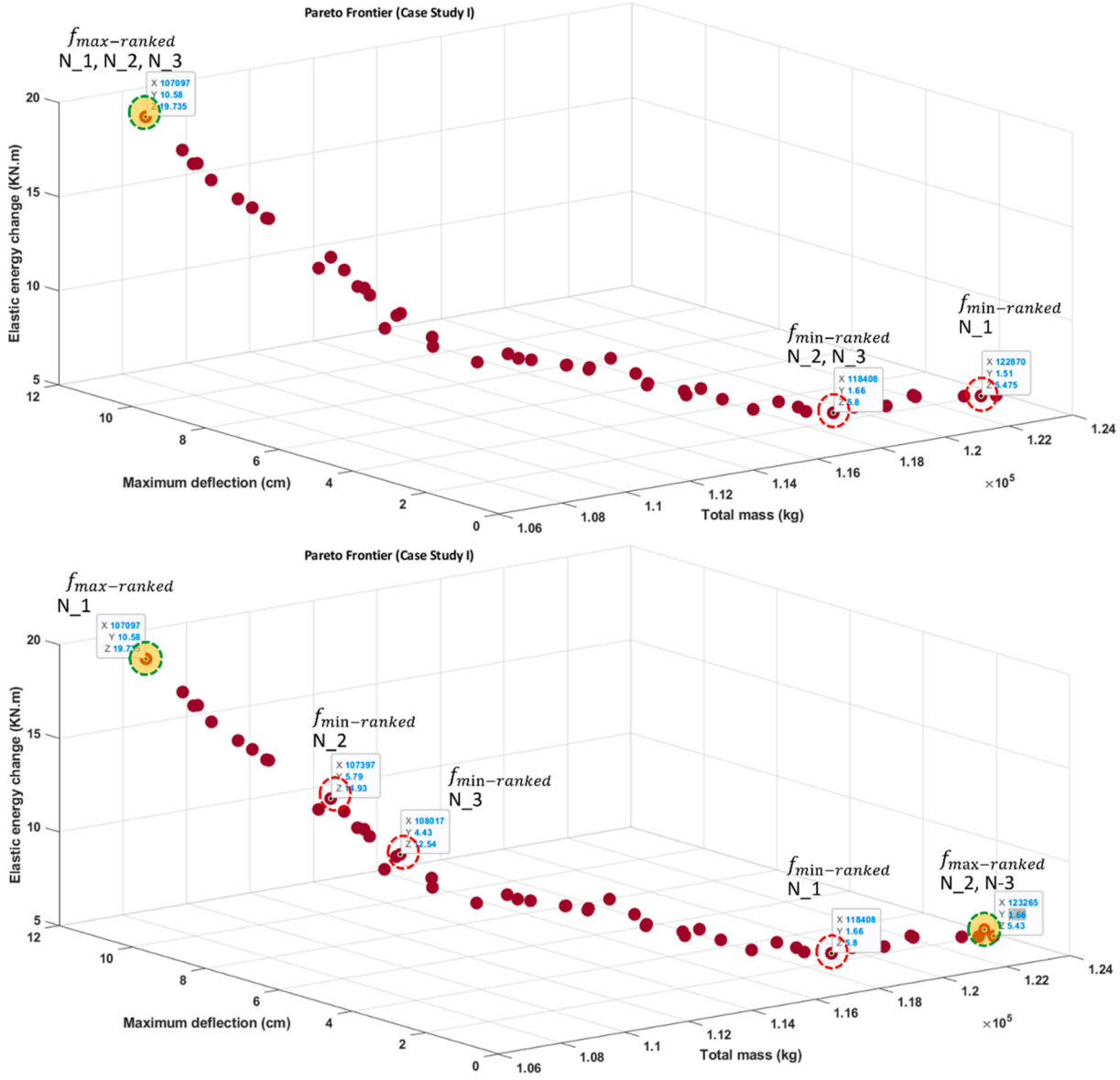

Fig. 14 The final best-chosen solution in case studies I, based on *j*1(top) and *j*2(bottom) from Table 18.

relationship between the normalization method and the final selected solution. Whichever normalization method is chosen should be kept consistent throughout the entire process to ensure a consistent result is provided.

4.6. Comparison of before and after optimization

By comparing the base model in which the parameters were set based on the Isler shell with the optimized model (Table 15,Table 16), it was revealed that when considering structural performance in case study I, by considering judgment Matrix-1, the total mass (f_1) in the optimized model ($f_{\max-\text{ranked}}$) was reduced 17% compared to the based model. In comparison, Maximum Deflection (f_2) and elastic energy change (f_3) increased by 55% and 45%, accordingly. However, if $f_{\min-\text{ranked}}$ is considered, the optimized model clearly outperforms the Isler model in all three objectives. This is evident as the total weight of the structure is reduced by 6%, the maximum deflection is reduced by 23%, and elastic energy change is nearly 42% lower in the optimized model. In case study I, when considering judgment Matrix-2, both $f_{\min-\text{ranked}}$ and $f_{\max-\text{ranked}}$ perform better than the base model.

In contrast, the $f_{\max-\text{ranked}}$ by employing judgment Matrix-1 has the same acoustic performances, Sound pressure level (f_7) and A-weighted SPL (f_8) in comparison to the base model. While both total weight (f_1) and the ratio of shell surface to covering the area (f_4) of the optimal solution increased by 13% in the optimal model.

In addition, while comparing the energy performance, the optimized model was significantly better performance; The surface area of the glazing (f_5) was 61% decreased (better performance), and the photovoltaic surface area on the exterior surface (f_9) increased by 13% in the optimized

Table 19 The minimum and maximum values of each objective that are used to scale the objective functions.

Objective function	Min	Max
f_1	107096.9	168278.2
f_2	1.44	84.95
f_3	5.43	450.88

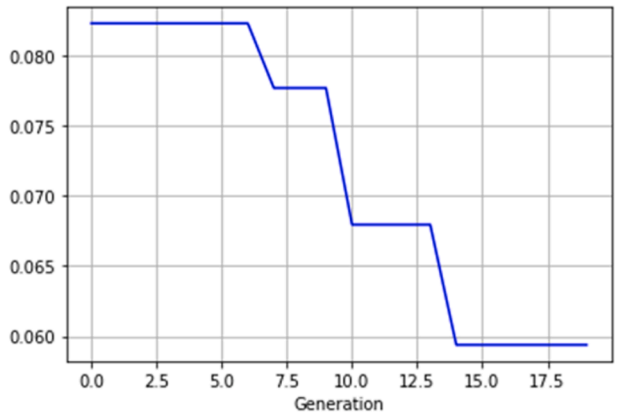

Fig. 15 The minimum of the WSM over the generation by employing GA.

model (f_9). Additionally, the total volume in the optimized solution was 10% less than the volume of the base model (Table 15, Table 16, Fig. 12).

It is important to note that user preferences are crucial in the final solution selection. If user preferences are more inclined toward structural, acoustic, or energy performance, a quite different optimal solution will be picked up from the Pareto front, highlighting the influence of user preferences in the decision-making process.

4.7. Comparison of the proposed method with the weighted sum method

In the weighted sum method, which is known as the weighted linear combination or simple additive weighting method, a weight should be determined and assigned to each objective, and the sum of these weights should be equal to one (Cucuzza et al., 2021; Mirjalili and Dong, 2020). A new objective function is constructed by combining all the objectives linearly. Here, a multi-objective problem is mapped to a single objective function, and a combination of variables is searched, which minimizes/maximizes the sum function. WSM is formulated in (Eq. (12)):

$$\overrightarrow{f\left(\vec{X}\right)} = \sum_{i=1}^{k} W_i f_i^{\text{norm}}\left(\vec{X}\right), \tag{12}$$

while: $\sum_{i=1}^{k} W_i = 1$.

The W_i is the determined weight for each objective, and the f_i^{norm} is the normalized objective.

To compare this method with the proposed method, in case study I, a new objective function is formulated using Eq. (12) and the assigned weights were calculated from judgment Matrix-1 (Eq. (8)). Then, using the same parametric model in case study I, and considering this formulated objective function (Eq. (13)), a genetic algorithm was utilized to search for the global optimum.

$$\overrightarrow{f\left(\vec{X}\right)} = \left[w_1 \cdot f_1\left(\vec{X}\right) + w_2 \cdot f_2\left(\vec{X}\right) + w_3 \cdot f_3\left(\vec{X}\right)\right];$$

$$w_{i-\text{norm}} = [0.11398 \quad 0.81421 \quad 0.07180]^T.$$

Then we will have

$$\overrightarrow{f\left(\vec{X}\right)} = \left[0.11398 \cdot f_1\left(\vec{X}\right) + 0.81421 \cdot f_2\left(\vec{X}\right) + 0.07180 \cdot f_3\left(\vec{X}\right)\right]. \tag{13}$$

To ensure that the objectives are comparable, objectives should be scaled (normalized) based on Eq. (14) and then combined. Without scaling, one objective with larger numerical values can dominate the optimization process, undermining the balance between the objectives (Kangazian and Pourghanbari, 2024; Nateghi and Kaczmarczyk, 2023).

$$f_i{}^{\sim}\left(\vec{X}\right) = f_i^{\text{norm}} = \frac{f_i\left(\vec{X}\right) - f_i^{\min}}{f_i^{\max} - f_i^{\min}}, \tag{14}$$

where $f_i{}^{\sim}(\vec{X})$ is the scaled objective, which lies in the range [0,1] ($= f_i^{\text{norm}}$), $f_i^{\max}$ and $f_i^{\min}$ are maximum and minimum values of $f_i(\vec{X})$.

The minimum and maximum values of each objective used to scale the objective functions are presented in the table below (Table 19).

The minimum value of the objective function in the weighted Sum method utilizing GA was found to be 0.057827, as reflected in Fig. 15, and the related values of the objective function (f_1 to f_3) are provided in Table 20. By putting the normalized values of f_1 to f_3 from Table 15 in Eq. (12), the value of the sum of the objective function will be computed as 0.03012 and 0.08147 by considering judgment Matrix-1 and putting values of $f_{\text{min-ranked}}$ and $f_{\text{min-ranked}}$ accordingly, which is different to the result found by WSM (0.05782), and close to the mean value of these two: $(0.03012 + 0.08147)/2$ that is equal to 0.055795.

In addition, the optimized solution found with the AHP method performed better than the one found by the WSM. While the total mass (f_1) was about the same, comparing the deflection (f_2) and elastic energy change (f_3) showed that the solution found with the AHP method was 76% and 5% lower (refer to $f_{\text{min-ranked}}$ in Table 15 and values found by the WSM method in Table 20).

Table 20 Values of f_1 to f_3 that make the objective function of the Weighted Sum Method minimum.

Objective function	Min
f_1	122806.37
f_2	4.25
f_3	12.36

Comparing these results with the AHP method using judgment matrix-1 showed that the proposed method of combining MOO and the AHP method could find better results overall in comparison to the WSM, which adds to the accuracy and credibility of the proposed methodology.

$$\overrightarrow{f\left(\vec{X}\right)}_{\min} = \left[0.11398 \cdot f_1\left(\vec{X}\right) + 0.81421 \cdot f_2\left(\vec{X}\right) + 0.07180 \cdot f_3\left(\vec{X}\right)\right] = 0.057827.$$

Furthermore, it should be noted that the challenge in employing the weighted sum method is that it is not easy to define the weights, whereas, in the integration of the MOO and AHP method, the consistency of the determined weights is checked (*CR*) to ensure the reliability in DM's determination. In addition, using the weighted sum method is that finding the global minimum is not always guaranteed.

4.8. Methodology limitations

Based on our observations, and because this method aims to rank and sort the solution, by using the NSGA-II, we can always provide the Pareto front, and the proposed method will rank it based on user preferences over the criteria (objective functions). Therefore, the final selected solution is optimal and can be used for further development. There is no right or wrong solution when picking from the Pareto front since all the solutions are optimal; thus, so far, we have not identified any limitations in implementing this method.

However, it is essential to note that tuning the values in the judgment matrix to achieve consistent preferences over the objective functions, particularly when the number of objective functions increases, is a complex and challenging task for inexperienced users. Additionally, the objective functions must be normalized with a proper method before the weight coefficient is applied, allowing them to be comparable.

5. Conclusion

The Pareto front solutions are a collection of optimal solutions that are superior to others and not dominated by one another. Selecting a solution from this collection of optimal alternatives for design development is essential. This research utilized a unique method by combining multi-objective optimization with the analytical hierarchy process (AHP). The solutions in the Pareto front are scored and ranked by constructing a judgment matrix, which indicates the DM's preferences over the objective functions. The DM's role is crucial as their preferences guide the ranking process. Two case studies were conducted to demonstrate the practical application and reliability of the proposed method. The main contributions of this research could be summarized as the following:

- Combining multi-objective optimization with the analytical hierarchy process takes the optimization method one step further and allows the decision-maker to interact more effectively in the process of finding the optimal solution. In this workflow, the DM's role in the design process will significantly increase, and the designer will be enabled to collaborate on the produced results more interactively.
- By integrating the MOO and AHP, the engineer or decision-maker (DM) is enabled to score, rank, and sort the solutions based on the project's requirements and preferences. The AHP method enables DM, a trade-off among various criteria, to solve a complex design problem.
- The advantages of this method are to conduct pairwise comparisons of the solutions using AHP to rank the solutions on the Pareto front. It involves structuring the problem into a hierarchy, comparing the solutions pairwise based on the decision-maker's preferences, and calculating a score for each solution. Thus, this tool can assist the decision-maker in organizing the solutions scientifically and according to the defined criteria.
- Despite other methods mentioned in this study, this method will always yield an optimal solution; in fact, this method will not affect the optimization process but will assist in ranking the solutions that are provided in the Pareto front, and DMs' will always evaluate the final solution, and if required, can easily shift to the other best next solutions and pick them for design development.
- It should be emphasized that AHP selects from the Pareto set produced by NSGA-II. Thus, the chosen solution retains Pareto-optimality. AHP does not—and cannot—move outside that optimal front or "improve" it in a mathematical sense; it simply encodes the DM's utilities to pick one solution.
- Consistency in a Decision Maker's (DM's) preferences is critical for valid judgment matrices in this method. The Consistency Ratio (*CR*) must be below 10% to ensure logical coherence. An example matrix presented in Sectio 4.3, with a *CR* of 256% revealed contradictions in the DM's rankings and by adjusting one value, the matrix achieved a *CR* of 1.2%, demonstrating how minor corrections can align preferences and ensure consistency. This underscores the need for rigorous validation of judgment matrices to avoid flawed decision-making.
- What should be noted here is that if the users have the same preferences over the criteria, they will end up picking the exact optimal solution from the Pareto front due to the same weights determined in the judgment matrix.
- This method can achieve different optimal solutions by structuring different judgment matrices, yet the architect's (DM's) preference has a direct impact on the final solutions. It is related to the DM and problem requirements and is unique for each problem set. However, it should be highlighted that this proposed method lets the DM select an optimal solution from the Pareto front and does not have any control or effect over the optimization process.
- The Study of the impact of the normalization method revealed that without standardization, the model might prioritize an objective function because the values are significantly larger (in this case, the total mass compared to deflection and elastic energy change) than the other values (objective functions). By standardizing, the two features are brought to the same scale, allowing for a more balanced analysis. However, more rigorous investigations are required to reveal the relation

between the normalization method and the final picked solution.
- The proposed method minimizes potential biases, even for inexperienced decision-makers (DMs), by focusing on preference-based selection rather than absolute correctness. The DM's role is to hierarchize criteria and express preferences, while the workflow scientifically guides the selection of an optimal solution from the Pareto front. Importantly, all solutions on the Pareto front are inherently optimal, differing only in how they trade off competing objectives. The DM's preferences simply steer the choice toward one of these equally valid solutions. If multiple users share identical preferences (reflected in the same judgment matrix weights), they will consistently select the same solution. Thus, the method ensures objective-driven decision-making without introducing bias, as every Pareto-optimal solution is superior to non-front alternatives.

This study lays the groundwork for ranking solutions on the Pareto front, offering a step toward utilizing decision-making tools in combination with the multi-objective optimization of continuous lightweight shell structures or any other multi-objective optimization problem.

6. Future research

Comparing the proposed method of combining MOO and the AHP with the other methods that were listed in Table 1, such as LINMAP, TOPSIS, the phased synergistic method, and other methods, to verify and compare the results. This will further reveal the method's potential pros and cons, as well as its limitations.

Additionally, existing topology optimization methods for shell structures can be discussed to illustrate how the proposed approach compares with direct topology or shape optimization methods in terms of computational cost, design flexibility, and performance.

In this study, nine objective functions were considered simultaneously for the optimization of lightweight shell structures, making it a complex case for optimization. Although considering more than three objective functions in shell structure optimal design is rare in the literature, it should be noted that future research may include other criteria such as "projected area" or "manufacturability."

Authorship contribution statement

MV: Conceptualization, Methodology, Formal analysis, Software, Data curation, Validation, Visualization, Writing - original draft, Writing - Review & Editing. **MG:** Project administration, Supervision, Writing - Review & Editing. **AE:** Supervision, Writing - Review & Editing. **MR:** Review & Editing. **PvB:** Supervision, Validation, Writing - Review & Editing.

Declaration of competing interest

The authors declare that they have no known competing financial interests or personal relationships that could have appeared to influence the work reported in this paper.

Acknowledgment

This publication was made possible with funding from the Taubman College of Architecture and Urban Planning at the University of Michigan. Additionally, the authors thank the support provided by the Department of Architectural Technology, Faculty of Architecture, College of Fine Arts, University of Tehran. We would like to appreciate the editorial and reviewers' feedback and insightful comments, which enhanced this manuscript.

Data availability

Here is a spreadsheet that formulates the AHP method for a three-by-three matrix. The inputs are DM's preferences over the objective functions (only three elements should be determined, and the other elements are determined based on the relation between elements, as mentioned in the method section). This spreadsheet calculates the *CR*, *CI*, λ_{max}, maximum eigenvalue, M_i and w_i for the matrix and performs the required checks. Additionally, this spreadsheet will calculate the normalized weight coefficient $(w_{i-\text{norm}})$.

Additionally, in another spreadsheet, the result (Pareto front) of Case Study I is reported. The users can construct a judgment matrix and calculate the weights using the first spreadsheet, then utilize it to rank and sort the Pareto front (with the second spreadsheet) based on their preferences (There are 125 unique matrices feasible for this case study). Moreover, this spreadsheet allows users to choose between three different methods of normalizing the values (objective functions), as discussed in Section 4.5. Any other data related to this research will be available upon request.

Appendix A. Supplementary data

Supplementary data to this article can be found online at https://10.1016/j.foar.2025.07.006.

References

Ali, A., Jayaraman, R., Azar, E., Maalouf, M., 2024. A comparative analysis of machine learning and statistical methods for evaluating building performance: a systematic review and future benchmarking framework. Build. Environ. 111268

Andreolli, F., Bragolusi, P., D'Alpaos, C., Faleschini, F., Zanini, M. A., 2022. An AHP model for multiple-criteria prioritization of seismic retrofit solutions in gravity-designed industrial buildings. J. Build. Eng. 45, 103493.

Ayman, A., Mansour, Y., Eldaly, H., 2024. Applying machine learning algorithms to architectural parameters for form generation. Autom. ConStruct. 166, 105624.

Baghdadi, A., Heristchian, M., Kloft, H., 2020. Displacement-based seismic assessment of heinz Isler's shell structures. Paper Presented at the Proceedings of IASS Annual Symposia.

Banti, N., Krawczyk, D.A., 2024. Integrating energy simulations and analytical hierarchy process procedure in multi-criteria evaluation of heating systems for industrial buildings. J. Build. Eng. 95, 110203.

Crespino, E., Adriaenssens, S., Fraddosio, A., Olivieri, C., Piccioni, M.D., 2024. A multi-objective optimization approach for novel shell/frame systems under seismic load. Paper Presented at the Structures.

Cucuzza, R., Costi, C., Rosso, M.M., Domaneschi, M., Marano, G.C., Masera, D., 2021. Optimal strengthening by steel truss arches in prestressed girder bridges. Paper Presented at the Proceedings of the Institution of Civil Engineers-Bridge Engineering.

Deb, K., Sindhya, K., Hakanen, J., 2016. Multi-objective optimization. In: Decision Sciences. CRC Press, pp. 161—200.

El-Bayeh, C.Z., Alzaareer, K., Brahmi, B., Zellagui, M., Eicker, U., 2021. An original multi-criteria decision-making algorithm for solar panels selection in buildings. Energy 217, 119396.

Goldbach, A.-K., Lázaro, C., 2024. CAD-Integrated parametric design and analysis of lightweight shell structures. Paper Presented at the Structures.

Gunantara, N., Ai, Q., 2018. A review of multi-objective optimization: methods and its applications. Cogent Eng. 5 (1), 1502242.

Guo, C., Bian, C., Liu, Q., You, Y., Li, S., Wang, L., 2022. A new method of evaluating energy efficiency of public buildings in China. J. Build. Eng. 46, 103776.

Ha, D.Q., Carstensen, J.V., 2023. Human-informed topology optimization: interactive application of feature size controls. Struct. Multidiscip. Optim. 66 (3), 59.

Henderi, H., Wahyuningsih, T., Rahwanto, E., 2021. Comparison of min-max normalization and Z-Score normalization in the K-nearest neighbor (kNN) algorithm to test the accuracy of types of breast cancer. Int. J. Intell. Inf. Syst. 4 (1), 13—20.

Hou, H.C., Wang, Y., Lan, H., 2023. Student residential apartment performance evaluation using integrated AHP-FCE method. J. Build. Eng. 67, 106000.

Kangazian, A., Pourghanbari, M., 2024. A many-objective optimization approach to design office building façade considering energy-daylight balance concept within prevalent climate types of Iran. J. Build. Eng. 98, 111234.

Kim, I.Y., de Weck, O.L., 2004. Adaptive weighted-sum method for bi-objective optimization: pareto front generation. Struct. Multidiscip. Optim. 29 (2), 149—158.

Kookalani, S., Cheng, B., Xiang, S., 2021. Shape optimization of GFRP elastic gridshells by the weighted lagrange ε-twin support vector machine and multi-objective particle swarm optimization algorithm considering structural weight. Structures. 33, October 2021, Pages 2066-2084.

Kumar, R., Singh, S., Bilga, P.S., Jatin, Singh, J., Singh, S., Pruncu, C.I., 2021. Revealing the benefits of entropy weights method for multi-objective optimization in machining operations: a critical review. J. Mater. Res. Technol. 10, 1471—1492.

Lazar, N., Chithra, K., 2021. Prioritization of sustainability dimensions and categories for residential buildings of tropical climate: a multi-criteria decision-making approach. J. Build. Eng. 39, 102262.

Li, Z., Lee, T.-U., Xie, Y.M., 2023. Interactive structural topology optimization with subjective scoring and drawing systems. Comput. Aided Des. 160, 103532.

Lin, C., Gao, F., Bai, Y., 2017. An intelligent sampling approach for metamodel-based multi-objective optimization with guidance of the adaptive weighted-sum method. Struct. Multidiscip. Optim. 57 (3), 1047—1060.

Mirjalili, S., Dong, J.S., 2020. Multi-Objective Optimization Using Artificial Intelligence Techniques. Springer.

Mueller, C.T., Ochsendorf, J.A., 2015. Combining structural performance and designer preferences in evolutionary design space exploration. Autom. ConStruct. 52, 70—82.

Mushtaha, E., Alsyouf, I., Al Labadi, L., Hamad, R., Khatib, N., Al Mutawa, M., 2020. Application of AHP and a mathematical index to estimate livability in tourist districts: the case of Al qasba in Sharjah. Front. Architect. Res. 9 (4), 872—889.

Nateghi, S., Kaczmarczyk, J., 2023. Multi-objective optimization of window opening and thermostat control for enhanced indoor environment quality and energy efficiency in contrasting climates. J. Build. Eng. 78, 107617.

Özerol, G., Arslan Selçuk, S., 2023. Machine learning in the discipline of architecture: a review on the research trends between 2014 and 2020. Int. J. Architect. Comput. 21 (1), 23—41.

Podvezko, V., 2009. Application of AHP technique. J. Bus. Econ. Manag. 10 (2), 181—189.

Ponsi, F., Bassoli, E., Vincenzi, L., 2021. A multi-objective optimization approach for FE model updating based on a selection criterion of the preferred Pareto-optimal solution. Paper Presented at the Structures.

Pugnale, A., 2018. Integrating form, structure and acoustics: a computational reinterpretation of frei otto's design method and vision. J. Int. Assoc. Shell Spatial Struct. 59 (1), 75—86.

Saaty, R.W., 1987. The analytic hierarchy Process—what it is and how it is used. Math. Model. 9 (3—5), 161—176.

Sangiorgio, V., Uva, G., Aiello, M.A., 2020. A multi-criteria-based procedure for the robust definition of algorithms aimed at fast seismic risk assessment of existing RC buildings. Paper presented Struct.

Talaei, M., Sangin, H., 2024. Thermal comfort, daylight, and energy performance of envelope-integrated algae-based bioshading and static shading systems through multi-objective optimization. J. Build. Eng. 90, 109435.

Teknomo, K., 2006. Analytic hierarchy process (AHP) tutorial. Revoledu. Com. 6, 1—20.

Thai, H.-T., 2022. Machine learning for structural engineering: a state-of-the-art review. Paper Presented at the Structures.

Vatandoost, M., Ekhlassi, A., Golabchi, M., Rahbar, M., von Buelow, P., 2024. Fabrication methods of shell structures. Autom. ConStruct 16.

Vatandoost, M., Golabchi, M., Ekhlassi, A., Rahbar, M., 2024a. Computational morphogenesis of lightweight continous concrete shell structures by utilizing metaheuristic algorithms. J. Int. Assoc.Shell Spatial Struct. https://doi.org/10.20898/j.iass.2024.007.

Vatandoost, M., Golabchi, M., Ekhlassi, A., Rahbar, M., 2024b. Topology and thickness optimization of concrete thin shell structures based on weight, deflection, and strain energy. Int. J. Eng. 37 (7), 1369—1383.

Xiao, Y., Yang, S., Xu, Z., Liao, W., Lu, Y., 2023. A human-machine collaboration frame in daylighting optimization of semi-outdoor space design by using phased synergistic method: a case study. J. Build. Eng. 79, 107879.

Xing, Y., Leng, J., Zhou, H., 2025. Cognitive preferences for architectural renovation strategies in traditional villages combining subjective evaluation and eye tracking. Front. Architect. Res. 11 (3), 561—573.

Xu, S., Chen, Y., Liu, J., Kang, J., Gao, J., Qin, Y., Li, G., 2024. Comprehensive improvement of energy efficiency and indoor environmental quality for university library atrium—A multi-objective fast optimization framework. Front. Architect. Res. 14 (4), 1017—1034.

Yan, X., Bao, D., Zhou, Y., Xie, Y., Cui, T., 2022. Detail control strategies for topology optimization in architectural design and development. Front. Architect. Res. 11 (2), 340—356.

Yu, B., Wu, S., Jiao, Z., Shang, Y., 2018. Multi-objective optimization design of an electrohydrostatic actuator based on a particle swarm optimization algorithm and an analytic hierarchy process. Energies 11 (9), 2426.

Yu, S., An, Y., Shi, C., Wang, A., 2024. Multi-objective hierarchical strategy for university dorm renovation in severe cold areas. J. Build. Eng. 91, 109660.

Yu, Z., Dai, H., Shi, Z., 2022. Structural form-finding of bending components in buildings by using parametric tools and principal stress lines. Front. Architect. Res. 11 (3), 561—573.

Zihao, M., Farouk, N., Singh, P.K., Abed, A.M., Samad, S., Babiker, S.G., Bouallegue, B., 2024. Multi-thermal recovery layout for a sustainable power and cooling production by biomass-based multi-generation system: techno-economic-environmental analysis and ANN-GA optimization. Case Stud. Therm. Eng. 105589